National Library of Canada
Acquisitions and Bibliographic Services Branch
395 Wellington Street
Ottawa, Ontario
K1A 0N4

Bibliothèque nationale du Canada
Direction des acquisitions et des services bibliographiques
395, rue Wellington
Ottawa (Ontario)
K1A 0N4

Your file Votre référence

Our file Notre référence

NOTICE

The quality of this microform is heavily dependent upon the quality of the original thesis submitted for microfilming. Every effort has been made to ensure the highest quality of reproduction possible.

If pages are missing, contact the university which granted the degree.

Some pages may have indistinct print especially if the original pages were typed with a poor typewriter ribbon or if the university sent us an inferior photocopy.

AVIS

La qualité de cette microforme dépend grandement de la qualité de la thèse soumise au microfilmage. Nous avons tout fait pour assurer une qualité supérieure de reproduction.

S'il manque des pages, veuillez communiquer avec l'université qui a conféré le grade.

La qualité d'impression de certaines pages peut laisser à désirer, surtout si les pages originales ont été dactylographiées à l'aide d'un ruban usé ou si l'université nous a fait parvenir une photocopie de qualité inférieure.

Canada

COMPUTATIONAL SOLUTIONS OF AERODYNAMIC PROBLEMS BASED ON A LAGRANGIAN FORMULATION

Pierre Nasrallah

Department of Mechanical Engineering

McGill University, Montréal

August 1994

A thesis submitted to the Faculty of Graduate Studies and Research in partial fulfillment of the requirements of the degree of Master of Engineering.

ISBN 0-612-05467-5

COMPUTATIONAL SOLUTIONS OF AERODYNAMIC PROBLEMS IN A LAGRANGIAN SYSTEM

TABLE OF CONTENTS

LIST OF FIGURES

Page

Abstract

The aerodynamic problems, involving the solution of the Euler equations of motion, are presently almost exclusively solved using an Euler formulation. This requires the generation of a spatial grid over which the problem is discretized. The grid generation process adds to the complexity to the problem being solved, especially in the case of complex body-shapes with flow discontinuities, such as shock waves and sliplines. Also, the Euler formulation is difficult to use for the aerodynamic problems of unspecified geometry.

A Lagrangian formulation permits to avoid the complexity of a grid generation while making it possible to obtain very accurate results. This Lagrangian formulation uses the stream function and Lagrangian distance to represent the flow instead of the Cartesian coordinates. Thus, the streamlines become coordinate lines in the Lagrangian formulation, which can easily represent complex body-shapes and sliplines, and is also more suitable to solve complex problems involving bodies of unspecified geometry.

This method was tested and validated against several test problems of specified geometry, including the supersonic flows with shock waves in a duct with a circular arc bump and past airfoils, as well as the flow in a nozzle. The solutions obtained with this Lagrangian method were found to be very accurate, displaying a high computational efficiency (actually providing second-order accuracy at a computational load of a first-order solution). Then, this Lagrangian method has been used to solve several aerodynamic problems with geometrically-unspecified body-shapes, such as (i) the determination of the geometry of a bump corresponding to a specified pressure distribution in supersonic flow, and (ii) the design of the geometry of a supersonic nozzle, based on the reflection-suppression condition, for a specified uniform flow at exit.

Résumé

La résolution des problèmes aérodynamiques, impliquants les équations du mouvement d'Euler, est presque exclusivement effectuée dans une formulation eulerienne. Cette formulation exige la génération d'un maillage spatial afin de discrétiser le problème à résoudre. La génération du maillage ajoute à la complexité du problème à résoudre, surtout dans le cas de modèles aux profiles compliqués, et des écoulements présentants des discontinuités, tel que des ondes de chocs ou des surfaces de glissement.

Il est à noter que la formulation eulerienne est difficile à appliquer aux problèmes aérodynamiques impliquants des parois à géométrie non déterminée *a priori*.

Une formulation lagrangienne permet d'éviter la génération du maillage, tout en produisant des résultats d'une précision élevée. Cette formulation lagrangienne décrit l'écoulement des fluides dans un système de coordonnés constitué des fonctions d'écoulements et de la "distance lagrangienne" au lieu des coordonnés cartésiennes. De telle sorte que dans la formulation lagrangienne les lignes d'écoulement deviennent références de coordonnés, ce qui facilite la description des modèles aux profiles complexes, et convient mieux aux problèmes impliquants des frontières géométriquement non définies.

Cette formulation a été testée et validée en l'apliquant à des problèmes types aux profiles définis, comprenant l'écoulement supersonique dans une soufflerie présentant un obstacle en arc de cercle sur une de ses parois, des profiles d'ailes et l'écoulement dans une tuyère. Les résultats obtenus s'avérèrent être d'une précision élevée, tout en affichant un rendement numérique supérieur.

Ensuite, cette formulation lagrangienne fut appliquée à la solution de différents problèmes aérodynamiques impliquants des modèles aux profiles non définis, tel que : (a) la détermination du profile d'un obstacle devant produire une répartition de pression définie sous l'effet d'un écoulement supersonique, (b) la conception d'une tuyère

supersonique, fondée sur la condition de non-reflection à la paroi, afin de produire un écoulement régulier à la sortie.

LIST OF SYMBOLS

τ	Time (in Lagrangian notation)
ξ	Lagrangian (material) coordinate
∇	Nabla operator. $\nabla = \mathbf{i}\frac{\partial}{\partial x} + \mathbf{j}\frac{\partial}{\partial y} + \mathbf{k}\frac{\partial}{\partial z}$
ρ	Density
α	Pressure ratio
σ	Oblique shock angle
θ	Flow direction angle
γ	Specific heat ratio of a gas (c_p/c_v)
Δ	Delta (incrementation symbol)
μ	Mach angle = $\sin^{-1}(1/M)$
A	Acceleration
a	Speed of sound
c_p	Specific heat at constant pressure
c_v	Specific heat at constant volume
δ_s	Shock wave thickness
h	Energy
i, j, k	Unit vector in the x, y, z direction
J	The Jacobian
λ	Length parameter along a streamline
M	Mach number
m	Mass flow rate
p	Pressure
R	Gas constant
r	Position vector

T	Temperature
t	Time (in Eulerian notation)
u	Velocity in the x direction
V	Velocity vector $\mathrm{V} = \mathrm{i}u + \mathrm{j}v$
V	Velocity
v	Velocity in the y direction
x	Position vector
x, y, z	Eulerian (spatial) coordinate

1. INTRODUCTION

In the last years the numerical methods for solving the flows of compressible fluids, both viscous and inviscid, have acquired a steadily increasing importance in the aeronautic industry and related fields. The fact is that these methods make it possible to obtain very accurate results about the flow at a fraction of the cost and time that would be required for experimenting in wind tunnels. A part of this effort has been directed toward the determination of inviscid supersonic flow field past bodies of various shapes for both steady and unsteady flows. The pressure field on the body surface, for instance, is of particular importance for the calculation of the forces and moments acting on it, which is needed to determine the performances of supersonic vehicles in flight.

Several methods have been developed for supersonic flows, most of which are aiming at solving the Euler equations based on an Eulerian representation, and integrating in time until the numerical convergence is reached. However, the Eulerian representation, which requires the generation of a geometrical grid over which the considered problem is solved, has a few limitations. The process of the grid generation itself is sensitive and has serious consequences on the results obtained. It is, for instance, difficult to fit a grid to some intricate body shapes. Some complex manipulations, such as conformal mapping, are often needed to adapt a grid to some difficult body shapes. This manipulations has an impact on the accuracy of the results. Also, some flow conditions, like shock waves, require complex manipulations and special treatments to capture the shape and position of the shock discontinuity. An example of such complex manipulation can be seen in the works of Ron-Ho Ni [18], Eidelman, Colella and Shreeve [6] and Mateescu and Lauzon [13]. Also the solution over the grid requires the addition of a dummy time-variable over which the problem would be solved iteratively. This process is rather computer-time consuming and tends to diminish the numerical accuracy.

The present work explores the possibilities offered by a new Lagrangian representation first introduced by Loh and Hui [11] to solve the same set of Euler equations in supersonic flows.

The Lagrangian representation method, which makes use of the streamlines and the Lagrangian time to describe the flow, eliminates the need for a complex grid and dummy time, permitting thus to obtain very accurate results in a fraction of the time usually required for solving in an Eulerian representation method.

The Lagrangian-time used in the Lagrangian representation is the real time of motion, as opposed to the dummy time used in the Eulerian representation. It is directly related to the distance traveled by the speed of motion. Together with the streamlines, the Lagrangian time provides for a complete description of the fluid flow.

The absence of a complex grid generation process offers many advantages over the Eulerian system. First it allows to save the time generally required to generate the grid and avoid the complex manipulations involved in fitting a grid to complex body shapes. Second it makes it possible to consider problems in which the body shape is not known. In this later case it becomes possible to compute the body shape provided we can supply a condition to which the flow is restricted. This condition could be the required pressure distribution on the unknown body shape. Thus we can compute the shape of a body that, when subjected to a particular flow, would generate a given pressure distribution. Another condition that can be applied to the flow is the reflection suppression condition to design the expansion section of a supersonic nozzle to produce a uniform flow at exit.

The Lagrangian representation has also the inherent property of correctly representing flow discontinuities, like shock waves, without requiring any particular treatments.

As we just described it, the Lagrangian representation in terms of Lagrangian-time and streamlines has a few limitations. The flux function is discontinuous across a slipline, and the system of equations constructed according to this representation is not fully

hyperbolic, being characterized by only five linearly independent eigenvectors, although the system possesses six real eigenvalues.

To overcome these problems a variant of the Lagrangian representation method that replaces the concept of Lagrangian-time described above by the Lagrangian-distance was first introduced by Hui and Zhao [9] and Yang and Hsu [27], in which the Lagrangian-distance is defined as the distance traveled by a particle along its streamline. These two entities are directly related, as the distance traveled is equal to the particle velocity multiplied by the elapsed time. The two procedures are equivalent but using the Lagrangian distance enables us to eliminate the potential deficiency in the Lagrangian representation of flows involving sliplines when represented using Lagrangian-time. It also proved to lead to more accurate results and to be faster.

The present work starts by developing the Euler equations in the Lagrangian representation. Then a numerical scheme is developed based on this Lagrangian formulation for the analysis of supersonic flows.

This numerical scheme is tested by solving a few classical two-dimensional problems, whose solution is known. Namely the cases of a simple supersonic nozzle build up from two parabolas smoothly connected and a tunnel flow with a circular arc bump on one of its sides. In both cases the Lagrangian method shows an excellent ability to produce very accurate results. Also, using the Lagrangian formulation it was possible to trace the streamlines shape.

The scheme based on Lagrangian representation proved to be very accurate and efficient. It also has shown a very good ability to solve for the flow discontinuities involved in the circular arc problem. The results obtained by the Lagrangian method were compared with analytical solutions and results previously published, for instance Ron-Ho Ni [18] and Eidelman, Colella and Shreeve [6]. Also, the program based on the Lagrangian formulation displayed a very high computational efficiency when compared to other work done in this department.

Next the Lagrangian scheme were applied to the slightly more difficult case of an airfoil in a supersonic flow. The cases considered included both flat and thick airfoils, with and without incidence.

Then, the Lagrangian scheme was used to compute the shape of a body for a specified pressure distribution [16]. For validation purpose, the specified pressure has been taken as the known pressure distribution for a flow past a circular arc bump. The results obtained were very accurate, the computed new shape being very close to the original circular one.

Finally, the Lagrangian scheme was applied to the problem of the expansion section of a supersonic nozzle design, with the condition of reflection suppression. It provided a very uniform flow at the nozzle exit.

2. GENERAL CONSIDERATIONS

2.1 Lagrangian representation versus Eulerian representation.

Most problems of gas dynamics amount to the solution of the Euler equations of motion. This set of equations is almost exclusively represented and solved using a Eulerian representation system, in which a fixed grid serves as a frame for the fluid motion.

In the Eulerian description of motion, the fluid properties such as velocity, pressure and density are determined at fixed points of space at each instant of time t, so that:

$$V = V(x, y, z, t),$$

$$\rho = \rho(x, y, z, t),$$

$$p = p(x, y, z, t),$$

where the flow properties (p, V, ρ, ...) are expressed in term of spatial coordinates (x, y, z) and time (t). In this representation, the flow properties (p, V, ρ, ...) belong to a fluid particle located at time t, at the considered spatial position (x, y, z).

The same set of Euler equations can be represented and solved in the Lagrangian representation system, in which the motion and properties of each fluid particle in the flow field is described as a function of initial position parameters (a, b, c) and the elapsed time referred to an initial time (t_0). At each instant t, the position (x, y, z) and other properties of each particle are given relatively to the initial position and time. It follows that in the Lagrangian representation the actual (physical) position (x, y, z) of a fluid particle is a variable property of that particle, like pressure and density, and is determined as a function of the fixed initial position and time,

$$x = x(a,b,c,t),$$

$$y = y(a,b,c,t),$$

$$z = z(a,b,c,t),$$

$$p = \Psi(a, b, c, t).$$

Pictorially we can figure the Eulerian representation to be the manner in which a static observer, viewing the fluid flow from a fixed location, would describe the fluid motion, whereas in Lagrangian notation one can imagine the observer identifying a fluid particle (or molecule) and following it (virtually riding upon it) along its trajectory.

The numerical simulation of inviscid compressible flow as modeled by the Euler equations of gas dynamics is an efficient method and is giving a satisfactory accuracy for flows without discontinuities, such as shock waves.

The approximative nature of this solution, and the fact that « The overall accuracy of numerical simulation is very closely related to the accuracy with which flow discontinuities are represented » [26], justifies the need for another type of solution, namely that based on a Lagrangian representation of the flow.

In the Lagrangian formulations based on stream function, the streamlines are coordinates lines. Consequently the flow tangency condition on a solid boundary is satisfied exactly on a streamline coordinate ($\xi=\xi_0$). Also note that since sliplines are also streamlines, they must be coordinate lines. This helps resolve sliplines better than Eulerian formulation.

Furthermore the streamlines and time lines possess much of the physics of the flow and are easily observable experimentally as they both are material lines.

2.2 The kinematics of fluid motion.

Kinematics is the description of motion per se. It takes no account of how the motion is generated or of the forces involved [21]. At some instant of time, we look at the fluid and remark that a certain particle is at a position ξ and later the same particle is at position x. We can take the first instant to be the time $t = 0$ and the later to be t; assuming that x is a function of t and the initial position ξ, we put:

$$\mathbf{x} = \mathbf{x}(\xi, t) ,$$

or (2.1)

$$x_i = x_i(\xi_1, \xi_2, \xi_3, t) ,$$

where the initial coordinates ξ of the particle will be referred to as the *material* or *Lagrangian coordinates*, which is itself defined in term of spatial or Eulerian coordinates (x_1, x_2, x_3). ξ should be thought of as a *particle label* and as such can be defined in any other way, for instance it can be defined in term of the streamlines as will be demonstrated in chapter 3.

The *spatial* or *Eulerian coordinate* (x, y, z) of the particle is its position or location. We will assume that the motion is continuous and single valued and that equation (2.1) can be inverted to give the initial position or Lagrangian coordinates of the particle corresponding to at any position $\mathbf{x}$ and time t:

$$\xi = \xi(\mathbf{x}, t) ,$$

or (2.2)

$$\xi_i = \xi_i(x_1, x_2, x_3, t) .$$

From this, we see that it is possible to define a coordinates transformation as follows:

$$(x, y, z) \Leftrightarrow (\xi, \eta, \tau) , \tag{2.3}$$

where ξ and η are components of the vector potential and τ is the Lagrangian time. In two-dimensional flows, the above transformation reduces to:

$$(x, y) \Leftrightarrow (\xi, \tau) , \tag{2.4}$$

where ξ is the stream function.

This means that a continuous string of particles does not break up during the motion or that the particles near a given particle remain in its neighborhood. By continuous

and single valued we mean that a particle cannot split up and occupy two locations at the same time nor can two distinct particles occupy the same location at the same time.

Equations (2.1) and (2.2) are related and demonstrate that the system is consistent, that is knowing the position (x) of a particle at a given time (t) we can determine its position at time t_0, or inversely that knowing its initial position ξ and time t we can deduct its position x.

The material (substantial) time derivative along a particle path of any of the flow parameters, f (such as ρ, u, v, p) is defined as:

$$\frac{Df}{Dt} = \left(\frac{df}{dt}\right)_p = \frac{\partial f}{\partial t} + u\frac{\partial f}{\partial x} + v\frac{\partial f}{\partial y} + w\frac{\partial f}{\partial z} = \frac{\partial f}{\partial t} + (\mathbf{V}\cdot\nabla)f \ , \tag{2.5}$$

where

$$u = \left(\frac{dx}{dt}\right)_p, v = \left(\frac{dy}{dt}\right)_p, w = \left(\frac{dz}{dt}\right)_p, \mathbf{V} = \left(\frac{d\mathbf{r}}{dt}\right)_p \ , \tag{2.6}$$

$$\mathbf{r} = \mathbf{i}x + \mathbf{j}y + \mathbf{k}z, \qquad \mathbf{V} = \mathbf{i}u + \mathbf{j}v + \mathbf{k}w \ , \tag{2.7}$$

and where $\frac{\partial f}{\partial t}$ is the local (partial) time derivative at a fixed point (for x, y, z constant), and

$$\mathbf{V}\cdot\nabla f = u\frac{\partial f}{\partial x} + v\frac{\partial f}{\partial y} + w\frac{\partial f}{\partial z} \ , \tag{2.8}$$

is the convective derivative.

For steady flows, the local time derivatives are zero ($\partial/\partial t=0$), and hence the material time derivative can be written as:

$$\frac{\partial f}{\partial \tau} = \frac{Df}{Dt} = u\frac{\partial f}{\partial x} + v\frac{\partial f}{\partial y} + w\frac{\partial f}{\partial z} = (\mathbf{V}\cdot\nabla)f \ , \tag{2.9}$$

where we introduce the notation τ to define the Lagrangian time for such steady flows.

The acceleration, or the material time derivative of the velocity, along the trajectory, is:

$$\mathbf{A} = \frac{d\mathbf{V}}{dt} = \frac{\partial \mathbf{V}}{\partial t} + (\mathbf{V} \cdot \nabla)\mathbf{V}, \tag{2.10}$$

In steady flow, this reduces to:

$$\mathbf{A} = (\mathbf{V} \cdot \nabla)\mathbf{V} = u\frac{\partial \mathbf{V}}{\partial x} + v\frac{\partial \mathbf{V}}{\partial y} + w\frac{d\mathbf{V}}{\partial z}\ . \tag{2.11}$$

2.3 Streamlines

A streamline is a line whose tangent at each instant of time and at any point in space gives the direction of the velocity of the fluid at that point. For steady flows, in which the velocity components are independent of time ($\partial u/\partial t=0$, $\partial v/\partial t=0$, $\partial w/\partial t=0$), the streamlines are identical with the path lines and streaklines (lines issued from the same point). The flow velocity being parallel to the streamline, there is no flow crossing the streamlines and thus the mass flow rate between two streamlines is constant.

For steady flows, the streamlines are defined as

$$\frac{d\mathbf{r}}{dt} = \mathbf{V}, \qquad \frac{dx}{u} = \frac{dy}{v} = \frac{dz}{w} = dt\ . \tag{2.12}$$

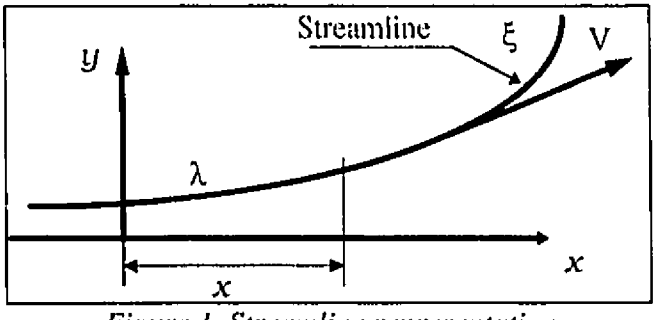

Figure 1. Streamline representation

3. EULER EQUATIONS OF MOTION IN LAGRANGIAN REPRESENTATION

3.1 Eulerian representation of the equations of motion.

The continuity, momentum and energy equations for the three-dimensional, steady flow of a compressible inviscid fluid in differential form are expressed as (Anderson [1], Shapiro [23])

$$\nabla \cdot (\rho \mathbf{V}) = 0 \,, \tag{3.1}$$

$$(\mathbf{V} \cdot \nabla)\mathbf{V} + \frac{1}{\rho}\nabla p = 0 \,, \tag{3.2}$$

$$\mathbf{V} \cdot \nabla\left(h + \frac{1}{2}V^2\right) = 0 \,, \tag{3.3}$$

where h represents the enthalpy, defined for an ideal fluid as

$$h = \frac{\gamma}{\gamma - 1}\frac{p}{\rho} = e + \frac{p}{\rho} \,. \tag{3.4}$$

For two-dimensional flows, they can be expressed in Cartesian coordinates as

$$\frac{\partial(\rho u)}{\partial x} + \frac{\partial(\rho v)}{\partial y} = 0 \,, \tag{3.5}$$

$$u\frac{\partial u}{\partial x} + v\frac{\partial u}{\partial y} + \frac{1}{\rho}\frac{\partial p}{\partial x} = 0 \,, \tag{3.6}$$

$$u\frac{\partial v}{\partial x} + v\frac{\partial v}{\partial y} + \frac{1}{\rho}\frac{\partial p}{\partial y} = 0 \,, \tag{3.7}$$

$$\frac{\partial}{\partial x}\left(\frac{V^2}{2}+\frac{\gamma}{\gamma-1}\frac{p}{\rho}\right)\rho u+\frac{\partial}{\partial y}\left(\frac{V^2}{2}+\frac{\gamma}{\gamma-1}\frac{p}{\rho}\right)\rho v=0\ . \tag{3.8}$$

3.2 The stream function

For two-dimensional steady flows, which represent the object of this analysis, the stream function, $\xi(x, y)$, is a point function defined in connection with the equation of continuity (3.5). Setting

$$u=\frac{\rho_0}{\rho}\frac{\partial \xi}{\partial y}\ , \tag{3.9}$$

and

$$v=-\frac{\rho_0}{\rho}\frac{\partial \xi}{\partial x}\ , \tag{3.10}$$

and replacing in the continuity equation we get:

$$\frac{\partial}{\partial x}\left(\rho_0\frac{\partial \xi}{\partial y}\right)+\frac{\partial}{\partial y}\left(-\rho_0\frac{\partial \xi}{\partial x}\right)=0\ , \tag{3.11}$$

which leads to

$$\frac{\partial}{\partial x}\left(\frac{\partial \xi}{\partial y}\right)=\frac{\partial}{\partial y}\left(\frac{\partial \xi}{\partial x}\right). \tag{3.12}$$

For a point function ξ, the order of differentiation is irrelevant (or Schwartz theorem holds), and thus the equation of continuity is the only required condition to the existence of the stream function ξ as a point function, which is defined as

$$\begin{aligned} d\xi &= \frac{\partial \xi}{\partial x}dx+\frac{\partial \xi}{\partial y}dy \\ &= \frac{1}{\rho_0}(\rho u dy-\rho v dx)\ . \end{aligned} \tag{3.13}$$

Computing the mass flow rate between two lines of constant ξ (see figure 2) we get:

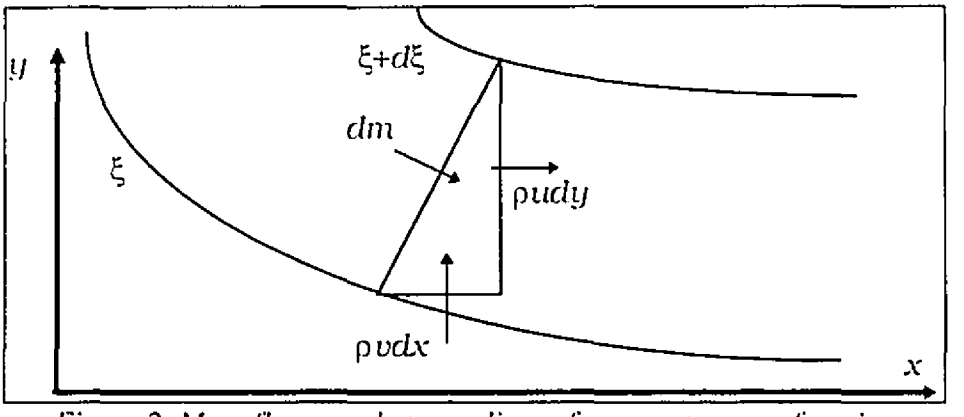

Figure 2. Mass flow rate between lines of constant stream function

$$d\dot{m} = \rho(u dy - v dx) . \tag{3.14}$$

Comparing equation (3.13) and (3.14) it becomes clear that:

$$d\dot{m} = \rho_0 d\xi , \tag{3.15}$$

which means that the change (variation) of the stream function ξ is a measure of the mass flow rate. It also means that a line of constant ξ does not admit any flow across itself. Hence, it follows that lines of constant ξ are also streamlines, since from equation (3.13) one can write

$$d\xi = 0 \quad \Rightarrow \quad \frac{dx}{u} = \frac{dy}{v} . \tag{3.16}$$

Considering a steady irrotational flow in a two-dimensional system:

$$f = f(\tau, \xi) , \tag{3.17}$$

where f is any fluid property represented as a function of the elapsed time τ and the Lagrangian coordinate ξ, such as the velocity components u and v, the fluid density, ρ,

and the pressure, p. Hence the position vector, r, and the fluid velocity, V, can be expressed as

$$\mathbf{r}(\tau,\xi) = \mathbf{i}\,x(\tau,\xi) + \mathbf{j}\,y(\tau,\xi)\,. \tag{3.18}$$

$$\mathbf{V}(\tau,\xi) = \frac{\partial \mathbf{r}}{\partial \tau} = \mathbf{i}u + \mathbf{j}v = \mathbf{i}\frac{\partial x}{\partial \tau} + \mathbf{j}\frac{\partial y}{\partial \tau}\,. \tag{3.19}$$

where

$$u(\tau,\xi) = \frac{\partial x}{\partial \tau}\,, \quad v(\tau,\xi) = \frac{\partial y}{\partial \tau}\,. \tag{3.20}$$

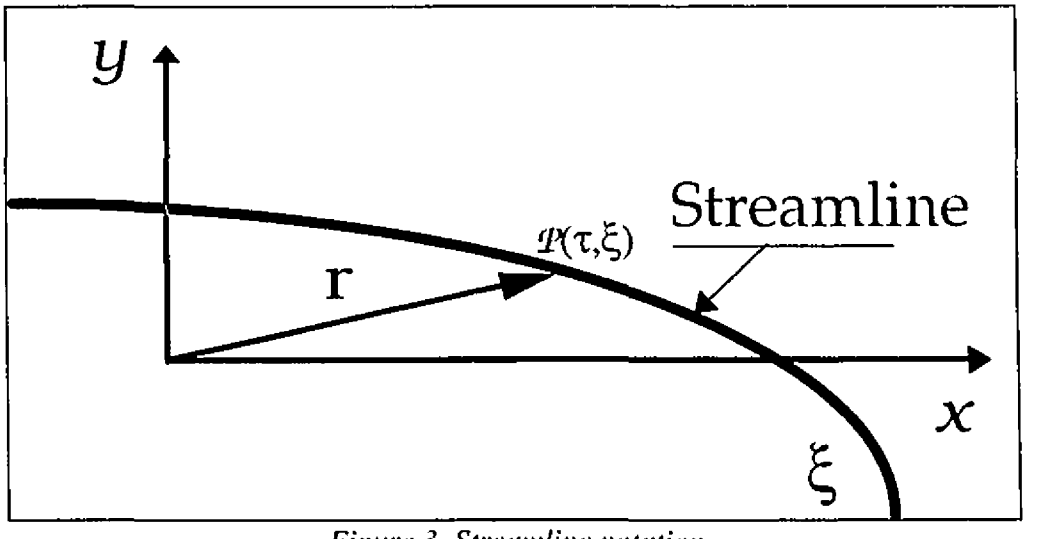

Figure 3. Streamline notation

For the two-dimensional flows, the material time-derivative can be expressed as

$$\frac{\partial f}{\partial \tau} = \frac{Df}{Dt} = (\mathbf{V}\cdot\nabla)f = u\frac{\partial f}{\partial x} + v\frac{\partial f}{\partial y}\,. \tag{3.21}$$

Considering the streamline definition

$$\xi = \xi(x,y)\,, \tag{3.22}$$

$$\frac{\partial \xi}{\partial x} = -\frac{\rho v}{\rho_0} , \tag{3.23}$$

$$\frac{\partial \xi}{\partial y} = \frac{\rho u}{\rho_0} , \tag{3.24}$$

one obtains successively:

$$\mathbf{V} \cdot \nabla \xi = u \frac{\partial \xi}{\partial x} + v \frac{\partial \xi}{\partial y} = u\left(-\frac{\rho v}{\rho_0}\right) + v\left(\frac{\rho u}{\rho_0}\right) = 0 , \tag{3.25}$$

and hence

$$\frac{1}{u}\frac{\partial \xi}{\partial y} = -\frac{1}{v}\frac{\partial \xi}{\partial x} = \frac{\rho}{\rho_0} = \frac{\rho}{K} . \tag{3.26}$$

where ρ_0 in equation (3.26) represents any reference value, which is primarily needed to balance the dimensions, and is arbitrarily chosen, so that one can replace it by K.

Replacing from equation (3.26) into equations (3.23) and (3.24) one can obtain

$$\frac{\partial \xi}{\partial y} = \frac{\rho u}{K} , \quad \frac{\partial \xi}{\partial x} = -\frac{\rho v}{K} . \tag{3.27}$$

These derivatives can be also expressed in terms of the Jacobian of the coordinates transformation (see equations (A.15) and (A.16) from Appendix A) as

$$\frac{\partial \xi}{\partial y} = \frac{u}{J} , \quad \frac{\partial \xi}{\partial x} = -\frac{v}{J} . \tag{3.28}$$

Comparing now the equations (3.27) and (3.28), in conjunction with equation (A.6) from Appendix A, one obtains successively

$$\frac{\rho}{K} = \frac{1}{J} , \quad \frac{K}{\rho} = J = \frac{\partial(x, y)}{\partial(\tau, \xi)} , \tag{3.29}$$

$$\frac{\partial x}{\partial \tau}\frac{\partial y}{\partial \xi} - \frac{\partial y}{\partial \tau}\frac{\partial x}{\partial \xi} = u\frac{\partial y}{\partial \xi} - v\frac{\partial x}{\partial \xi} : \tag{3.30}$$

a derivation for equation (3.29) can be obtained from the following equation, shown in Batchelor [30],

$$\frac{\partial(x,y,z)}{\partial(a,b,c)} = \frac{\rho_0}{\rho} \quad \text{or} \quad \frac{\partial(x,y)}{\partial(\xi,\tau)} = \frac{\rho_0}{\rho}.$$

Introducing now the notations

$$U = \frac{\partial x}{\partial \xi}\ , \quad V = \frac{\partial y}{\partial \xi}\ , \tag{3.31}$$

where U and V can be considered as the Cartesian components of the vector W

$$\mathbf{W} = \frac{\partial \mathbf{r}}{\partial \xi} = \mathbf{i}\frac{\partial x}{\partial \xi} + \mathbf{j}\frac{\partial y}{\partial \xi} = \mathbf{i}U + \mathbf{j}V\ , \tag{3.32}$$

in the same way in which x and y, or u and v are the components of the vectors r or V

$$\mathbf{r}(\tau,\xi) = \mathbf{i}x(\tau,\xi) + \mathbf{j}y(\tau,\xi)\ , \tag{3.33}$$

$$\mathbf{V} = \frac{\partial \mathbf{r}}{\partial \tau} = \mathbf{i}\frac{\partial x}{\partial \tau} + \mathbf{j}\frac{\partial y}{\partial \tau} = \mathbf{i}u + \mathbf{j}v\ , \tag{3.34}$$

since r is a point function, according to Schwartz theorem one can write:

$$\frac{\partial}{\partial \xi}\left(\frac{\partial \mathbf{r}}{\partial \tau}\right) = \frac{\partial}{\partial \tau}\left(\frac{\partial \mathbf{r}}{\partial \xi}\right), \tag{3.35}$$

where

$$\frac{\partial}{\partial \xi}\left(\frac{\partial \mathbf{r}}{\partial \tau}\right) = \mathbf{i}\frac{\partial u}{\partial \xi} + \mathbf{j}\frac{\partial v}{\partial \xi}\ , \tag{3.36}$$

$$\frac{\partial}{\partial \tau}\left(\frac{\partial \mathbf{r}}{\partial \xi}\right) = \mathbf{i}\frac{\partial U}{\partial \tau} + \mathbf{j}\frac{\partial V}{\partial \tau} \,. \tag{3.37}$$

one results

$$\left.\begin{aligned} \frac{\partial u}{\partial \xi} &= \frac{\partial U}{\partial \tau} \,, \\ \frac{\partial v}{\partial \xi} &= \frac{\partial V}{\partial \tau} \,. \end{aligned}\right\} \tag{3.38}$$

These equations are called the **compatibility relations**, defining the coordinates transformation between the Eulerian and Lagrangian formulations.

Referring to equation (3.29) we can also write:

$$\frac{K}{\rho} = J = \frac{D(x,y)}{D(\tau,\xi)} = \frac{\partial x}{\partial \tau}\frac{\partial y}{\partial \xi} - \frac{\partial x}{\partial \xi}\frac{\partial y}{\partial \tau} = uV - Uv \,, \tag{3.39}$$

considering the equations (3.20), the equations (A.10) and (A.11) in appendix A can be recast in the form:

$$\frac{\partial \tau}{\partial x} = \frac{1}{J}\frac{\partial y}{\partial \xi} = \frac{\rho}{K}\frac{\partial y}{\partial \xi} = \frac{\rho}{K}V \,, \tag{3.40}$$

$$\frac{\partial \tau}{\partial y} = -\frac{1}{J}\frac{\partial x}{\partial \xi} = -\frac{\rho}{K}\frac{\partial x}{\partial \xi} = -\frac{\rho}{K}U \,. \tag{3.41}$$

By definition one can write

$$\left.\begin{aligned} \frac{\partial}{\partial x} &= \frac{\partial \tau}{\partial x}\frac{\partial}{\partial \tau} + \frac{\partial \xi}{\partial x}\frac{\partial}{\partial \xi} \\ \frac{\partial}{\partial y} &= \frac{\partial \tau}{\partial y}\frac{\partial}{\partial \tau} + \frac{\partial \xi}{\partial y}\frac{\partial}{\partial \xi} \end{aligned}\right\} , \tag{3.42}$$

and replacing from equations (3.20), (3.23), (3.24), (3.32), (A.10) and (A.11) into equation (3.42) one obtains

$$\left.\begin{aligned}\frac{\partial}{\partial x}&=\frac{\rho}{K}\left[V\frac{\partial}{\partial\tau}-v\frac{\partial}{\partial\xi}\right]\\ \frac{\partial}{\partial y}&=\frac{\rho}{K}\left[-U\frac{\partial}{\partial\tau}+u\frac{\partial}{\partial\xi}\right]\end{aligned}\right\}. \tag{3.43}$$

from which one can write

$$\begin{aligned}\nabla\cdot\mathbf{f}&=\frac{\partial f_x}{\partial x}+\frac{\partial f_y}{\partial y}\\ &=\frac{\rho}{K}\left[V\frac{\partial f_x}{\partial\tau}-v\frac{\partial f_x}{\partial\xi}-U\frac{\partial f_y}{\partial\tau}+u\frac{\partial f_y}{\partial\xi}\right]\\ &=\frac{\rho}{K}\left[\frac{\partial}{\partial\tau}\left(Vf_x-Uf_y\right)-\frac{\partial}{\partial\xi}\left(vf_x-uf_y\right)-f_x\left(\frac{\partial V}{\partial\tau}-\frac{\partial v}{\partial\xi}\right)+f_y\left(\frac{\partial U}{\partial\tau}-\frac{\partial u}{\partial\xi}\right)\right]\end{aligned} \tag{3.44}$$

where f_x and f_y are the components of f in the x and y directions respectively.

Replacing from equation (3.38) into equation (3.44) and simplifying one obtains

$$\nabla\cdot\mathbf{f}=\frac{\partial f_x}{\partial x}+\frac{\partial f_y}{\partial y}=\frac{\rho}{K}\left[\frac{\partial}{\partial\tau}\left(Vf_x-Uf_y\right)-\frac{\partial}{\partial\xi}\left(vf_x-uf_y\right)\right], \tag{3.45}$$

and setting $\mathbf{f}=\rho\mathbf{V}=\mathbf{i}\rho u+\mathbf{j}\rho v$ and simplifying one obtains

$$\nabla\cdot(\rho\mathbf{V})=\frac{\partial(\rho u)}{\partial x}+\frac{\partial(\rho v)}{\partial y}=\frac{\rho}{K}\left[\frac{\partial}{\partial\tau}\rho(Vu-Uv)\right]. \tag{3.46}$$

3.3 Lagrangian representation of Euler equations of motion using Lagrangian time.

3.3.1 Continuity equation for steady flow

The continuity equation (3.1) will hence become

$$\nabla\cdot(\rho\mathbf{V})=\frac{\rho}{K}\left[\frac{\partial}{\partial\tau}(\rho(Vu-Uv))\right]=0\,, \tag{3.47}$$

and replacing from equations (3.29) and (3.32) one obtains

$$\nabla\cdot(\rho V)=\frac{\rho}{K}\left[\frac{\partial K}{\partial \tau}\right]=0\ , \tag{3.48}$$

and hence

$$\frac{\partial K}{\partial \tau}=0 \quad \text{or} \quad K=K(\xi)\ . \tag{3.49}$$

Equation (3.49) means that K is a function of ξ only, hence one can write

$$K=\rho(uV-vU)\ , \tag{3.50}$$

equation (3.49), in conjunction with equation (3.50), defines the continuity equation in Lagrangian formulation based on Lagrangian time.

3.3.2 Momentum equation for steady flow in lagrangian representation.

The momentum equation (3.2) in the Eulerian formulation in Cartesian coordinates has the following component equations in the x and y directions

$$u\frac{\partial u}{\partial x}+v\frac{\partial u}{\partial y}+\frac{1}{\rho}\frac{\partial p}{\partial x}=0\ , \tag{3.51}$$

$$u\frac{\partial v}{\partial x}+v\frac{\partial v}{\partial y}+\frac{1}{\rho}\frac{\partial p}{\partial y}=0\ , \tag{3.52}$$

replacing from equations (3.20) and (3.42) the first equation (3.51) can be expressed

$$\frac{\partial x}{\partial \tau}\left(\frac{\partial u}{\partial \tau}\frac{\partial \tau}{\partial x}+\frac{\partial u}{\partial \xi}\frac{\partial \xi}{\partial x}\right)+\frac{\partial y}{\partial \tau}\left(\frac{\partial u}{\partial \tau}\frac{\partial \tau}{\partial y}+\frac{\partial u}{\partial \xi}\frac{\partial \xi}{\partial y}\right)+\frac{1}{\rho}\left(\frac{\partial p}{\partial \tau}\frac{\partial \tau}{\partial x}+\frac{\partial p}{\partial \xi}\frac{\partial \xi}{\partial x}\right)=0\ , \tag{3.53}$$

simplifying one obtain

$$J\frac{\partial u}{\partial \tau}+\frac{1}{\rho}\frac{D(p,y)}{D(\tau,\xi)}=0\ , \tag{3.54}$$

or

$$K\frac{\partial u}{\partial \tau}+\frac{D(p,y)}{D(\tau,\xi)}=0\ . \tag{3.55}$$

Similarly, the second equation (3.52) can be expressed in the form:

$$K\frac{\partial v}{\partial \tau}+\frac{D(x,p)}{D(\tau,\xi)}=0\ . \tag{3.56}$$

Equations (3.55) and (3.56) together represent the momentum equation for steady flow in Lagrangian formulation using Lagrangian time.

3.3.3 Energy equation for steady flow.

The energy equation (3.3) can be written in the following form

$$\mathbf{V}\cdot\nabla\left(\frac{\gamma}{\gamma-1}\frac{p}{\rho}+\frac{1}{2}\left(u^2+v^2\right)\right)=0\ , \tag{3.57}$$

where

$$\mathbf{V}\cdot\nabla=u\frac{\partial}{\partial x}+v\frac{\partial}{\partial y}=\frac{\partial x}{\partial \tau}\frac{\partial}{\partial x}+\frac{\partial y}{\partial \tau}\frac{\partial}{\partial y}\ , \tag{3.58}$$

hence we can rewrite equation (3.57) as follows

$$\begin{aligned}&\frac{\partial x}{\partial \tau}\frac{\partial}{\partial x}\left[\frac{\gamma}{\gamma-1}\frac{p}{\rho}+\frac{1}{2}\left(\frac{\partial x}{\partial \tau}\right)^2+\frac{1}{2}\left(\frac{\partial y}{\partial \tau}\right)^2\right]+\\&\frac{\partial y}{\partial \tau}\frac{\partial}{\partial y}\left[\frac{\gamma}{\gamma-1}\frac{p}{\rho}+\frac{1}{2}\left(\frac{\partial x}{\partial \tau}\right)^2+\frac{1}{2}\left(\frac{\partial y}{\partial \tau}\right)^2\right]=0\end{aligned}\ , \tag{3.59}$$

rearranging we get

$$\begin{aligned}&\frac{\partial x}{\partial \tau}\left[\frac{\gamma}{\gamma-1}\frac{1}{\rho^2}\left(\rho\frac{\partial p}{\partial x}-p\frac{\partial \rho}{\partial x}\right)+u\frac{\partial u}{\partial x}+v\frac{\partial v}{\partial x}\right]+\\&\frac{\partial y}{\partial \tau}\left[\frac{\gamma}{\gamma-1}\frac{1}{\rho^2}\left(\rho\frac{\partial p}{\partial y}-p\frac{\partial \rho}{\partial y}\right)+u\frac{\partial u}{\partial y}+v\frac{\partial v}{\partial y}\right]=0\end{aligned}\ , \tag{3.60}$$

simplifying and rearranging we get

$$\frac{\partial}{\partial \tau}\left(\frac{1}{2}(u^2+v^2)+\frac{\gamma}{\gamma-1}\frac{p}{\rho}\right)=0 \tag{3.61}$$

Equation (3.61) defines the energy equation for steady flow in Lagrangian formulation using Lagrangian time.

3.4 Euler equations in Lagrangian formulation based on Lagrangian-time

We now can write the Euler equations of motion using the Lagrangian representation (equations 3.49, 3.55, 3.56 and 3.61) developed in section 3.3 in the following matrix form

$$\frac{\partial E}{\partial \tau}+\frac{\partial F}{\partial \xi}=0\ , \tag{3.62}$$

where

$$E=\begin{vmatrix} K \\ H \\ Ku+pV \\ Kv-pU \\ U \\ V \end{vmatrix}=\begin{vmatrix} e_1 \\ e_2 \\ e_3 \\ e_4 \\ e_5 \\ e_6 \end{vmatrix} \quad \text{and} \quad F=\begin{vmatrix} 0 \\ 0 \\ -pv \\ pu \\ -u \\ -v \end{vmatrix}=\begin{vmatrix} f_1 \\ f_2 \\ f_3 \\ f_4 \\ f_5 \\ f_6 \end{vmatrix} \tag{3.63}$$

and

$$\begin{aligned} U&=\frac{\partial x}{\partial \xi}, \qquad V=\frac{\partial y}{\partial \xi}\ , \qquad H=\frac{1}{2}(u^2+v^2)+\frac{\gamma}{\gamma-1}\frac{p}{\rho}, \\ u&=\frac{\partial x}{\partial \tau}, \qquad v=\frac{\partial y}{\partial \tau}, \qquad K=\rho(uV-vU)\ , \end{aligned} \tag{3.64}$$

where: the equation related to e_1 represents the continuity equation, the equation related to e_2 represents the energy equation, the equations related to e_3 and e_4 represent the

momentum equations and the equations related to C_+ and C_- are the compatibility equations (see equation 3.38).

Equation (3.62) represents Euler equations in Lagrangian formulation based on Lagrangian-time, using (τ, ξ) as independent variables.

3.5 Euler equations in Lagrangian formulation based on Lagrangian-distance

The Lagrangian representation based on Lagrangian-time developed in section 3.4 has two deficiencies as noted by Hui and Zao [9] and Yang and Hsu [27]. First the flux function *(F)* in equation (3.62) is discontinuous across a slipline. This is a consequence to the fact that the tangential component of fluid velocity is discontinuous across a slipline, while the pressure p and the flow direction angle θ are continuous. Second the system of equation represented by equation (3.62) is not fully hyperbolic. In the sense that although this system has six real eigenvalues, it only has five linearly independent eigenvectors associated with them.

In order to correct this problem the following transformation is introduced:

$$dx = \frac{u}{\mathbf{V}^{\alpha}} d\lambda + U d\xi \,, \tag{3.65}$$

$$dy = \frac{v}{\mathbf{V}^{\alpha}} d\lambda + V d\xi \,, \tag{3.66}$$

where α is an arbitrary constant, V is the fluid velocity and ξ is the streamline.

$$\mathbf{V} = \sqrt{u^2 + v^2} \,. \tag{3.67}$$

Setting $d\xi$=0, and replacing in equations (3.65) and (3.66) we get:

$$\frac{dx}{u} = \frac{dy}{v} = \frac{d\lambda}{\mathbf{V}^{\alpha}} \,, \tag{3.68}$$

from which it follows that λ is a variable along the streamline.

Setting $\alpha = 0$ and $d\xi=0$ we get:

$$\frac{dx}{d\lambda} = u \ , \tag{3.69}$$

$$\frac{dy}{d\lambda} = v \ , \tag{3.70}$$

from which it follows that when α is equal to zero, λ is equivalent to the Lagrangian time.

Setting $\alpha = 1$ and $d\xi=0$ we get:

$$dx = \frac{u}{\mathbf{V}} d\lambda \ , \tag{3.71}$$

$$dy = \frac{v}{\mathbf{V}} d\lambda \ , \tag{3.72}$$

$$dx^2 + dy^2 = \left(\frac{u^2}{\mathbf{V}^2} + \frac{v^2}{\mathbf{V}^2} \right) d\lambda^2 = d\lambda^2 \ , \tag{3.73}$$

from which it follows that when α is equal to one, λ is equivalent to the distance traveled by a particle along its streamline, which we will call the Lagrangian distance.

Substituting equations (3.65) and (3.66) in equations (3.47), (3.51), (3.52) and (3.57), going through the substitution process of section 3.3, and setting α equal to one, we get:

$$\frac{\partial E}{\partial \lambda} + \frac{\partial F}{\partial \xi} = 0 \ , \tag{3.74}$$

where

$$E = \begin{vmatrix} K \\ H \\ Ku + pV \\ Kv - pU \\ U \\ V \end{vmatrix} = \begin{vmatrix} e_1 \\ e_2 \\ e_3 \\ e_4 \\ e_5 \\ e_6 \end{vmatrix} \quad \text{and} \quad F = \begin{vmatrix} 0 \\ 0 \\ -p\sin\theta \\ p\cos\theta \\ -\cos\theta \\ -\sin\theta \end{vmatrix} = \begin{vmatrix} f_1 \\ f_2 \\ f_3 \\ f_4 \\ f_5 \\ f_6 \end{vmatrix} \tag{3.75}$$

where θ is the flow direction angle, and

$$\begin{aligned} U &= \frac{\partial x}{\partial \xi}, \qquad V = \frac{\partial y}{\partial \xi}, \qquad H = \frac{1}{2}(u^2 + v^2) + \frac{\gamma}{\gamma - 1}\frac{p}{\rho}, \\ u &= \frac{\partial x}{\partial \tau}, \qquad v = \frac{\partial y}{\partial \tau}, \qquad K = \rho(uV - vU). \end{aligned} \tag{3.76}$$

where: the equation related to e_1 represents the continuity equation, the equation related to e_2 represents the energy equation, the equations related to e_3 and e_4 represent the momentum equations and the equations related to e_5 and e_6 are the compatibility equations (see equation 3.38). Equations (3.74) represents Euler equations in Lagrangian formulation based on Lagrangian-distance, using (λ, ξ) as independent variables, it is functionally equivalent to equations system (3.62). By considering these two equation systems, (3.62) and (3.74) we note that:

- Although the streamlines and time lines are non-orthogonal in the physical plane the resulting transformed equations remain very simple.
- The Lagrangian method of computation is also self contained without need of re-mapping to the Eulerian space.
- The Lagrangian time τ in equation (3.62) is a true time variable of motion, as distinguished from any time-like variable (fictitious time) in the Eulerian formulation. Marching in τ means following the fluid particles along their path. Thus the computation method follows exactly the particle movements even when it crosses a shock wave where flow direction changes abruptly. (A cell is exactly a fluid particle and remains intact at all time).

4. NUMERICAL PROCEDURE

We will now develop a numerical strategy to solve the equations systems (3.62) and (3.74). It should be noted that those two systems are equivalent and similar, so that the same strategy applies to both of them. The differences, which appear in the flux function F, are small and are solved effectively with the same procedure. Also at the programming level, the same program, with minor modifications, is used to solve both systems.

4.1 Space discretization

Consider the inlet of the expansion section of a supersonic nozzle shown in figure 4. We set up an incoming supersonic uniform flow as shown, and we will discretize this flow in the Lagrangian plane (τ-ξ) or (λ-ξ). This incoming flow is set parallel to the walls, which are straight and parallel in the inlet section. So that we know the streamlines at this section to be straight and parallel. We choose a line at the inlet section perpendicular to the wall, and thus to the streamlines at this section, and identify it as the time line τ=0 in the Lagrangian plane τ-ξ (or λ=0 in the λ-ξ plane). We will identify a line ξ=0 on the lower wall, as shown in figure 4, and parametrize the line τ=0 (or λ=0) in term of streamlines ξ ($\xi_0 = 0, \xi_1, \xi_2, \ldots, \xi_n$). By definition we know that the mass flow rate between two streamlines is constant (see section 2.3), hence each streamline can be identified by the mass flow rate between it and the reference streamline (the line ξ=0). The streamlines being equally spaced, it is possible to define an interval $\Delta\xi$ as the mass flow rate between any two streamlines as follows

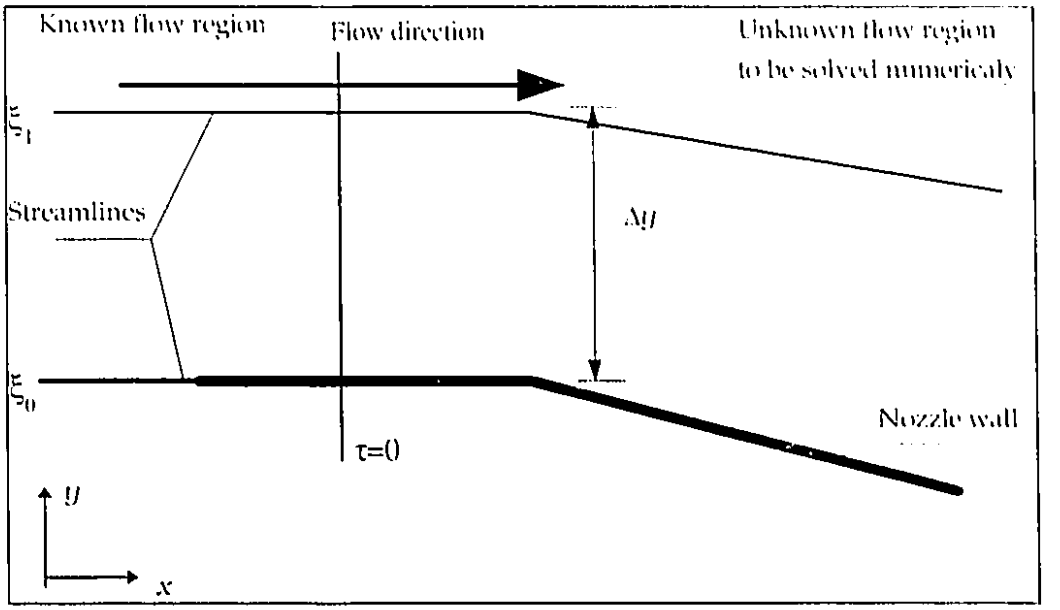

Figure 4. Nozzle inlet section (enlarged)

$$\Delta\xi = \rho u \cdot \Delta y \cdot L \,, \tag{4.1}$$

where L is the system width, which is assumed unity.

The increments in the τ (or λ) direction are computed at every step in order to satisfy the stability (CFL) condition as follows

$$\Delta\tau = \frac{\Delta\xi \mathrm{CFL}}{2\rho u_j^2 \tan(\theta+\mu)_j} \,, \tag{4.2}$$

$$\Delta\lambda = \frac{\Delta\xi \mathrm{CFL}}{2\rho u_j \tan(\theta+\mu)_j \cos\theta_j} \,, \tag{4.3}$$

where

$$\mu = \sin^{-1}\frac{1}{M} \,, \tag{4.4}$$

and θ is the flow direction angle (see Appendix F).

4.2 Initialization

The start-up or initial values of all the variables used in the program are computed from the inlet value of the flow and the geometry of the inlet section as described here: we compute the compatibility relations

$$\frac{\Delta y}{\Delta \xi} = \frac{1}{\rho u L} = V^0 = \frac{\partial y}{\partial \xi} , \tag{4.5}$$

the flow being uniform and parallel to the x axis there is no variation of ξ relative to x. then we can write

$$\frac{\partial x}{\partial \xi} = 0 = U^0 , \tag{4.6}$$

where the superscript 0 indicates the initial time step (τ=0 or λ=0).

We can now compute all the e and F function at τ=0 as follows:

$$\begin{aligned}
e_1^0 &= K^0 = \rho\left(u^0 V^0 - v^0 U^0\right) , \\
e_2^0 &= H^0 = \frac{1}{2}\left(\left(u^0\right)^2 + \left(v^0\right)^2\right) + \frac{\gamma}{\gamma - 1}\frac{p^0}{\rho^0} , \\
e_3^0 &= K^0 u^0 + p^0 V^0 , \qquad e_4^0 = K^0 v^0 - p^0 U^0 , \\
e_5^0 &= U^0 , \qquad\qquad e_6^0 = V^0 ,
\end{aligned} \tag{4.7}$$

the e function computed in equation (4.7) are valid for both the Lagrangian formulations based on Lagrangian-time and on Lagrangian-distance. We also compute the flux in the Lagrangian formulation based on Lagrangian-time

$$\begin{aligned}
f_1^0 &= 0 , \qquad f_2^0 = 0 , \\
f_3^0 &= -p^0 v^0 , \qquad f_4^0 = p^0 u^0 , \\
f_5^0 &= -u^0 , \qquad f_6^0 = -v^0 ,
\end{aligned} \tag{4.8}$$

or in the Lagrangian formulation based on Lagrangian-distance

$$
\begin{aligned}
f_1^0 &= 0\,, & f_2^0 &= 0\,,\\
f_3^0 &= -p^0 \sin\theta^0\,, & f_4^0 &= p^0 \cos\theta^0\,,\\
f_5^0 &= -\cos\theta^0\,, & f_6^0 &= -\sin\theta^0\,,
\end{aligned}
\tag{4.9}
$$

the flux functions of equation (4.8) are used in the system based on the Lagrangian-time (τ-ξ), while the flux functions of equation (4.9) are used with the system based on the Lagrangian-distance formulation (λ-ξ). In this later case the angle θ represents the flow direction angle at inlet and usually set equal to zero.

4.3 The computational mesh

The computational mesh in the τ-ξ (or λ-ξ) plane is shown in figure 5. The mesh is naturally rectangular, i.e. no special manipulations are needed to transform it to a rectangular shape. Although the streamlines *j*, *j+1*,... are neither straight nor parallel, their Lagrangian representation is naturally rectangular. This is easy to figure if we consider that the distance Δξ separating two streamlines represents a streamline incrementation, and in this implementation equals the mass flow rate between any two streamlines ($\Delta\xi=\rho u L \Delta y$)[1] , which is constant regardless of the actual shape of the streamlines. So that any two (or more) streamlines represented in Lagrangian coordinates (τ-ξ), or (λ-ξ), will appear as straight and parallel lines. Also τ represents the time elapsed since the moment τ=0, so that lines of constant τ will be parallel and will yield a rectangular (τ, ξ) mesh. In the formulation based on Lagrangian-distance (λ-ξ), the same reasoning applies to the distance-step lines. Incrementing in λ, which represents the distance traveled along each streamline, taking an equal distance increment Δλ for all the streamlines, will produce the same pattern of straight and parallel lines.

The superscript *n* refers to the time step number and subscript *j* refers to the cell number.

---

[1] *L* is the width of the system (tunnel) and is set equal to unity for a two-dimensional system.

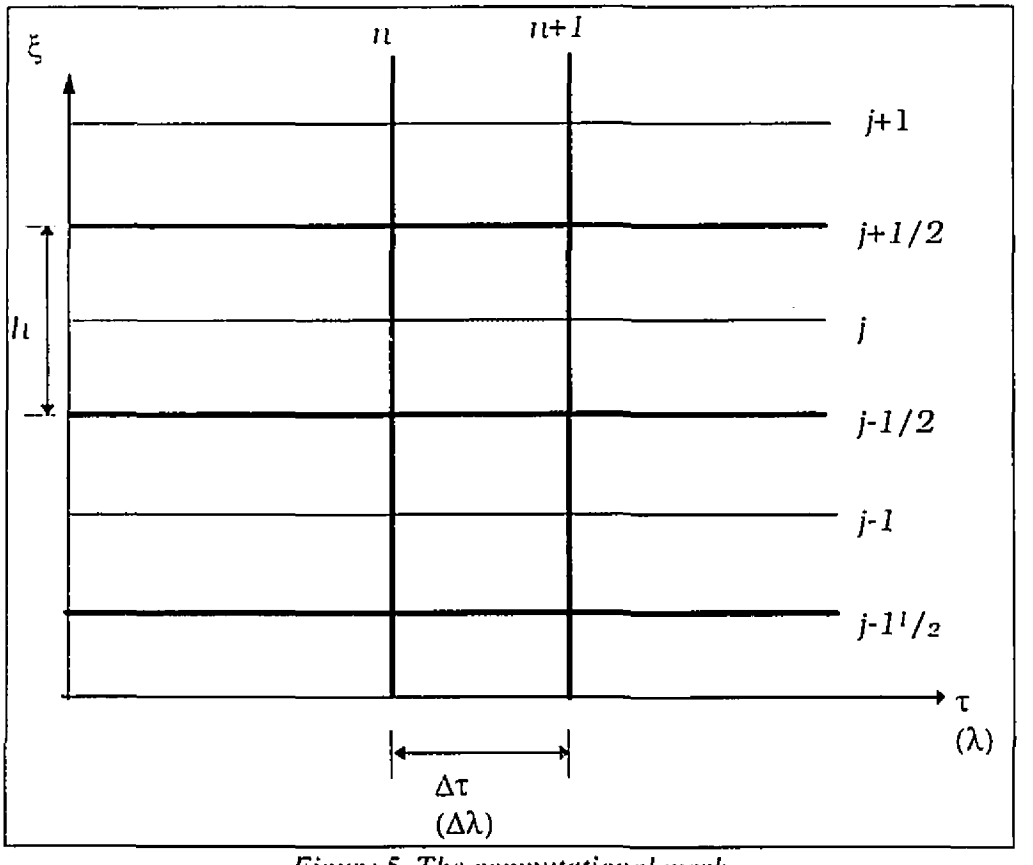

Figure 5. The computational mesh

The mesh divides the computational domain into cells which are centered in the ξ direction at ξ_j and at $\tau^{n+1/2}$ (or $\lambda^{n+1/2}$), and have a uniform height h as follows

$$h = \Delta\xi_j = \xi_{j+1/2} - \xi_{j-1/2} \,. \tag{4.10}$$

The difference equation for the j^{th} cell at time step n using Lagrangian-time is derived by integrating equation (3.62) as follows:

$$E_j^{n+1} = E_j^n - \frac{\Delta\tau^n}{\Delta\xi_j}\left(F_{j+1/2}^{n+1/2} - F_{j-1/2}^{n+1/2}\right), \tag{4.11}$$

or for the solution in using on Lagrangian-distance based on equation (3.74), we get

$$E_j^{n+1} = E_j^n - \frac{\Delta\lambda^n}{\Delta\xi_j}\left(F_{j+1/2}^{n+1/2} - F_{j-1/2}^{n+1/2}\right). \tag{4.12}$$

4.4 Method of solution

The flow domain is discretized into a mesh in terms of streamlines ξ and time lines τ or λ (see figure 5). We assume that we are at a given instant $\tau=n\Delta\tau$ (or $\lambda=n\Delta\lambda$) and that at this instant all the flow properties are known. (In fact we start at $\tau=0$ and progress numerically to $\tau=\tau^n$). From this point we want to compute all the properties at $\tau=\tau^{n+1}$ (or $\lambda=\lambda^{n+1}$). To do this we need to solve the equations set (4.11) or (4.12).

From this point on the discussion will mention only the Lagrangian-time formulation, the same procedure being applicable also to the Lagrangian-distance formulation.

We consider the cell labeled j (shown shaded in figure 5). The process is then repeated for all the cells.

We start by computing the flux values at $\tau=\tau^{n+1/2}$, on the two bounding streamlines $j+1/2$ and $j-1/2$ $\left(f_{j+1/2}^{n+1/2} \text{ and } f_{j-1/2}^{n+1/2}\right)$. We will start by assuming that at $\tau=\tau^n$ the flow properties are constant within each cell (e.g. the pressure is constant between the points $j-1/2$ and $j+1/2$ and is equal to the pressure value at j). The solving process is similar to Riemann problem, i.e. we imagine that at the instant $\tau=\tau^n$ there are two cells of gas at different states (j and $j-1$) separated by a membrane at $j-1/2$. This membrane separating the two cells is removed at the instant $\tau=\tau^n$ (instantly), and we want to compute the interaction along the streamline $j-1/2$ (See figure 6).

Since the line $j-1/2$ is itself a streamline between j and $j-1$, the pressure and flow direction at $j-1/2$ and $n+1/2$ must be the same on its both sides. The situation shown in figure 6 assumes that the pressure p_j^n is greater than p_{j-1}^n, then a shock wave propagates into cell $j-1$ and an expansion fan into cell j.

To start the solution process we make a guess for the pressure p at $j-1/2$ and $n+1/2$, let

$$\alpha = \frac{p_{j-1/2}^{n+1/2}}{p_{j-1}^n}, \tag{4.13}$$

for this value of α we compute the flow direction angle at j-$^1/_2$ and n+$^1/_2$ using the oblique shock relation developed in Appendix C as follows

$$\theta^{n+1/2}_{j-1/2} = \theta^{n}_{j-1} - \tan^{-1}\left[\frac{\alpha - 1}{\gamma\left(M^{n}_{j-1}\right)^2 - \alpha + 1}\cdot\sqrt{\frac{2\gamma\left(M^{n}_{j-1}\right)^2}{(\gamma+1)\alpha+\gamma-1} - 1}\right]. \tag{4.14}$$

Then for the same guessed pressure value p at j-$^1/_2$ and n+$^1/_2$, let

$$\tilde{\alpha} = \frac{p^{n+1/2}_{j-1/2}}{p^{n}_{j}}\ , \tag{4.15}$$

solving for the expansion fan propagating into cell j, we first compute the Mach number at j-$^1/_2$ and n+$^1/_2$ using the isentropic relation

$$\left(\tilde{M}^{n+1/2}_{j-1/2}\right)^2 = \frac{2}{\gamma-1}\left(\frac{1+\frac{\gamma-1}{2}\left(M^{n}_{j}\right)^2}{\tilde{\alpha}^{\frac{\gamma-1}{\gamma}}} - 1\right), \tag{4.16}$$

and then compute the flow direction angle at j-$^1/_2$ and n+$^1/_2$ using the characteristic relations detailed in Appendix E

$$\tilde{\theta}^{n+1/2}_{j-1/2} = \theta^{n}_{j} + \nu\left(M^{n}_{j}\right) - \nu\left(\tilde{M}^{n+1/2}_{j-1/2}\right)\ , \tag{4.17}$$

where ν is the Prandtl-Meyer expansion function

$$\nu(M) = \sqrt{\frac{\gamma+1}{\gamma-1}}\tan^{-1}\left(\sqrt{\frac{\gamma-1}{\gamma+1}}\sqrt{M^2-1}\right) - \tan^{-1}\sqrt{M^2-1}\ . \tag{4.18}$$

The values of the flow direction angle θ at j-$^1/_2$ and n+$^1/_2$ computed with equations (4.14) and (4.17) should be equal as they lie on the same streamline. If they are not equal an iterative process is applied to get the value of $p^{n+1/2}_{j-1/2}$ that will produce the same flow direction θ at j-$^1/_2$ and n+$^1/_2$ with equations (4.14) and (4.17).

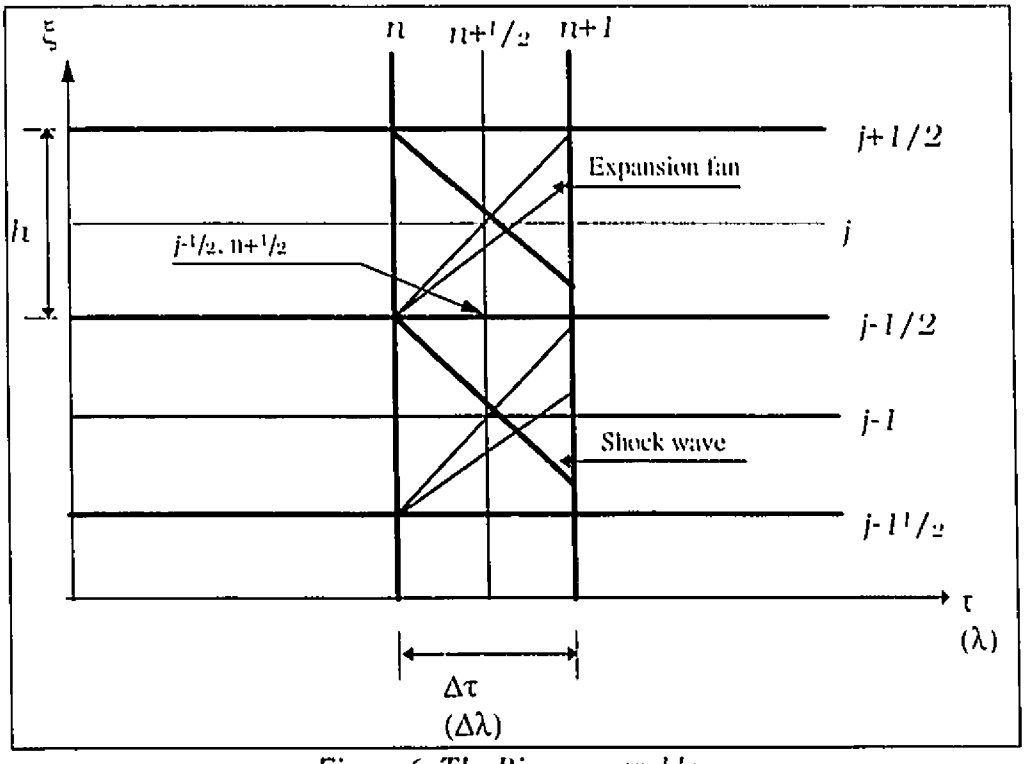

Figure 6. The Riemann problem

When the value of p and θ are determined, we use these values to compute the fluxes (equation 4.8 or 4.9) which we use in equation (4.11) to determine the values of E at the next time step $\tau=\tau^{n+1}$.

4.5 Computing the flux for the formulation based on Lagrangian-time

In order to compute the flux for the formulation based on Lagrangian-time (equation 4.8), we note that we need the flow velocity at the point considered (j-1/2 and n+1/2). The interface at j-1/2 being a slipline the velocity on its both sides can vary and hence must be computed separately through the oblique shock and the expansion fan. In both cases we start by computing the Mach number and density at (j-1/2 and n+1/2).

Through the oblique shock wave we get using the Rankine-Hugoniot relation

$$M_{j-\frac{1}{2}}^{n+\frac{1}{2}} = \sqrt{\frac{\left(M_{j-1}^{n}\right)^2\{(\gamma+1)\alpha+\gamma-1\}-2(\alpha^2-1)}{\alpha\{(\gamma-1)\alpha+\gamma+1\}}}\,, \tag{4.19}$$

and

$$\frac{\rho_{j-1/2}^{n+1/2}}{\rho_j^n} = \frac{(\gamma+1)\alpha+\gamma-1}{(\gamma-1)\alpha+\gamma+1}, \tag{4.20}$$

where α is the pressure ratio through the oblique shock computed with equation (4.13).

Through the expansion fan we use the Mach number value obtained from the isentropic relation (4.16) and compute the corresponding density

$$\frac{\tilde{\rho}_{j-1/2}^{n+1/2}}{\rho_j^n} = \tilde{\alpha}^{\frac{1}{\gamma}}, \tag{4.21}$$

where $\tilde{\alpha}$ is the pressure ratio through the expansion fan computed with equation (4.15).

Then we can compute the velocity as follows

$$V = M\sqrt{\frac{\gamma p}{\rho}}, \tag{4.22}$$

and the velocity components

$$u = V\cos\theta, \tag{4.23}$$

$$v = V\sin\theta, \tag{4.24}$$

where θ is the flow direction angle.

4.6 Boundary considerations

We note at this point that in order to progress from $\tau=n\Delta\tau$ to $\tau=(n+1)\Delta\tau$ we need two flux values $\left(f_{j+1/2}^{n+1/2} \text{ and } f_{j-1/2}^{n+1/2}\right)$, so that each streamline (or cell) j needs the interaction of the two streamlines surrounding it to be solved. However this description method fails at the system wall boundaries, where the streamlines bounding the system are delimited by the system's walls. Thus we need a special method to take into account the

first and last streamlines at the bounding walls. This problem has two possible solutions, which are described in the following sections:

4.6.1 Bounding streamlines recessed from the wall.

In order to maintain the logic we locate the first (and last) streamline of the system at a distance $\nabla\xi/2$ away from the bounding wall, in such a way that this streamline be located in the middle of a cell bounded by two streamlines. The outer bounding streamline being located on the boundary wall. This fact is a consequence of the tangency condition between the bounding wall and the last streamline. Thus the direction (θ) of this streamline is identical to that of the wall and known. The iteration procedure described in the preceding section is used to compute only the pressure at the wall, i.e. we iterate to match the angle θ obtained with equation (4.14) or (4.17) with the wall direction at $j=1/2$ and $n+1/2$.

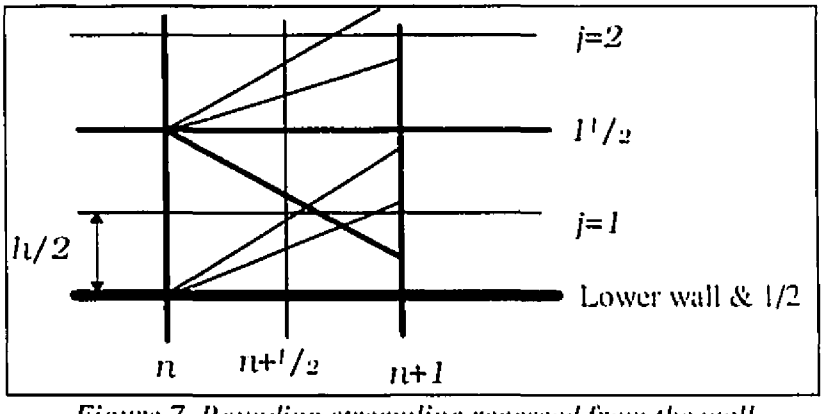

Figure 7. Bounding streamline recessed from the wall

4.6.2 Bounding flow represented by an image flow.

An alternate procedure is to position the first and last streamlines exactly on the bounding walls. In this case we use an image flow outside the wall to provide for the external cell with which the last streamline will interact. This case is represented in figure 8, where the limiting streamline (here streamline number 1) is positioned on the wall itself. The image flow being the image of the second streamline (j=2).

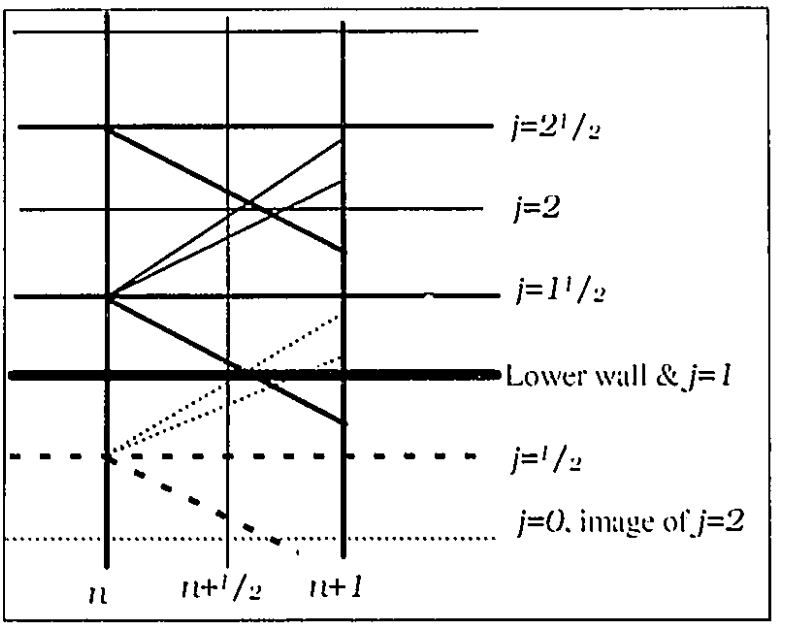

Figure 8. Image bounding streamline

We need to compute the flux through the imaginary streamline, at $j=1/2$ and $n+1/2$, as shown in figure 8. This is done using the procedure described in section 4.4.

5. SPECIFIC FLOW PROBLEMS SOLVED USING THE LAGRANGIAN APPROACH.

5.1 Specified geometry problems

In this section the Lagrangian approach is applied to some conventional problems of aerodynamics. By conventional problems, we mean problems where we compute the effect of the interaction of a gas flow with a body or variable shape duct, and that the contour of the body or duct subjected to the flow is known.

5.1.1 Flow in a tunnel with a circular arc bump.

This problem consists of a straight tunnel with a circular arc bump on one of its surface, as shown in figure 9. The bump has a maximum thickness of 4% its length located at its middle. This is a standard problem for which known solutions exist (see Ron-Ho Ni [18] and Eidelman, Colella and Shreeve [6]), that will be used to validate the results obtained with the Lagrangian formulation. Figure 11 shows the Mach number distribution along the tunnel for the lowest and highest streamlines (the two streamlines closest to the lower and upper wall respectively), and for three intermediate streamlines. The streamlines are numbered from the lowest up, i.e. the streamline closest to the lower wall is the streamline number 1, and the one closest to the upper wall has the number of the last streamline in the solution (in this case 61). This problem was solved in both the Lagrangian-time based and Lagrangian-distance based formulations using the boundaries streamlines recessed from the wall as described in section 4.6.1. Figure 11 also shows a the results obtained using the Lagrangian formulation compared with those obtained by Eidelman, Colella and Shreeve [6], which are superimposed on the line for the lowest and highest streamlines. Figure 12 shows a comparison of the results obtained with the two variants of the Lagrangian formulation (based on Lagrangian-distance and Lagrangian-time).

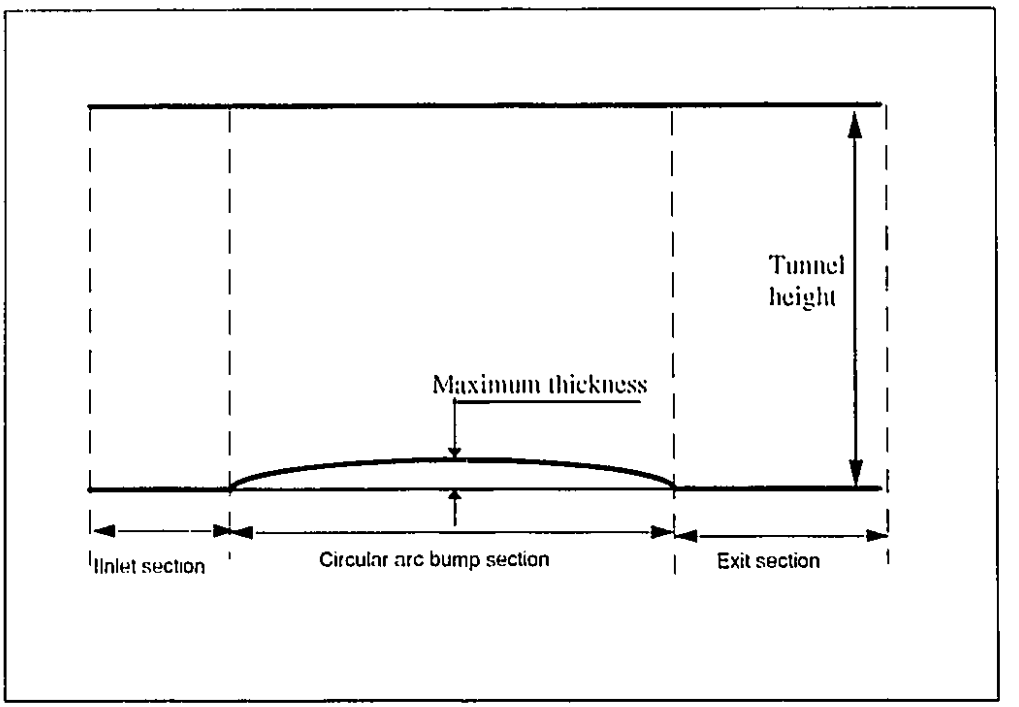

Figure 9. Circular arc bump problem

This problem involves sudden changes in flow direction at the wall, specifically at the two sharp corners at the junction between the circular arc bump and the tunnel wall. In supersonic flows this situation generates an oblique shock, or a Prandtl-Meyer expansion. Special care is taken at this points to maintain the accuracy of the system across the shock wave (or expansion wave). This is done by adjusting the distance $\Delta\lambda$ (in the system using the Lagrangian-time notation $\Delta\tau$), so that the turning point lies exactly on a cell boundary line, λ or τ line (see figure 10). This ensures that the shock (or expansion) will be issued at a cell corner.

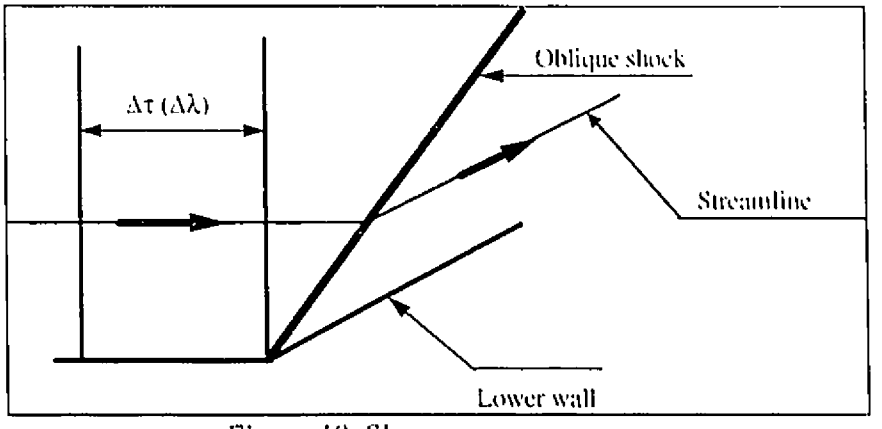

Figure 10. Sharp corner treatment

The problem was solved for an inlet mach number of 1.65, 61 equally spaced streamlines, the total tunnel length was 3 divided in three equal sections and the tunnel height was equal to 1. The maximum thickness of the circular bump was 4% of its length.

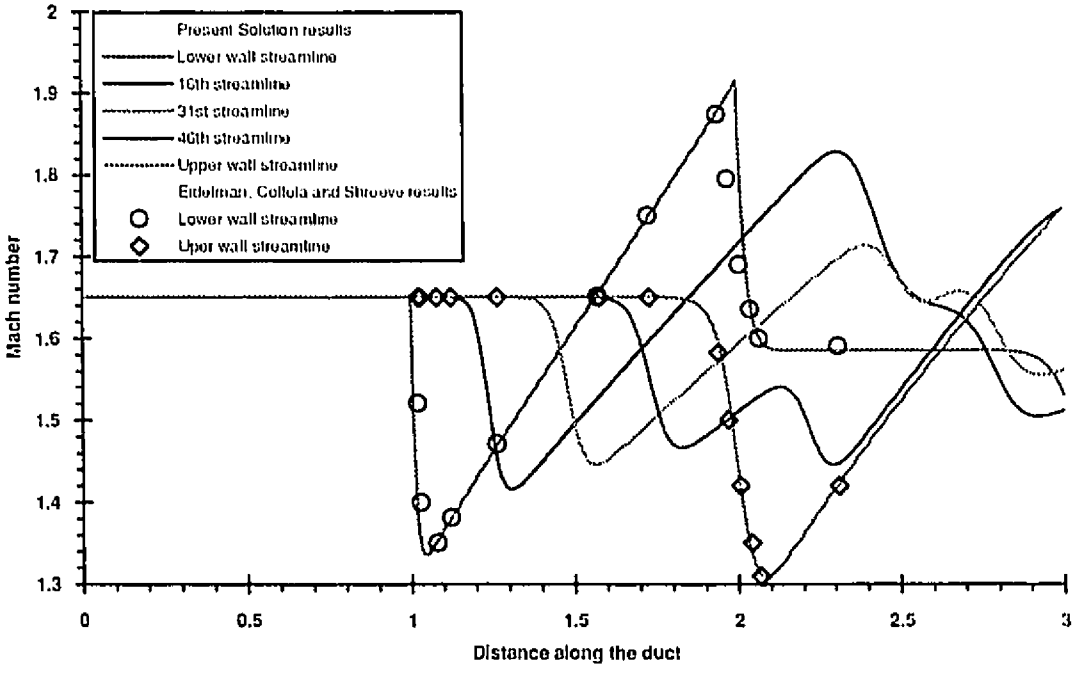

Figure 11. Mach number distribution for the circular arc bump problem

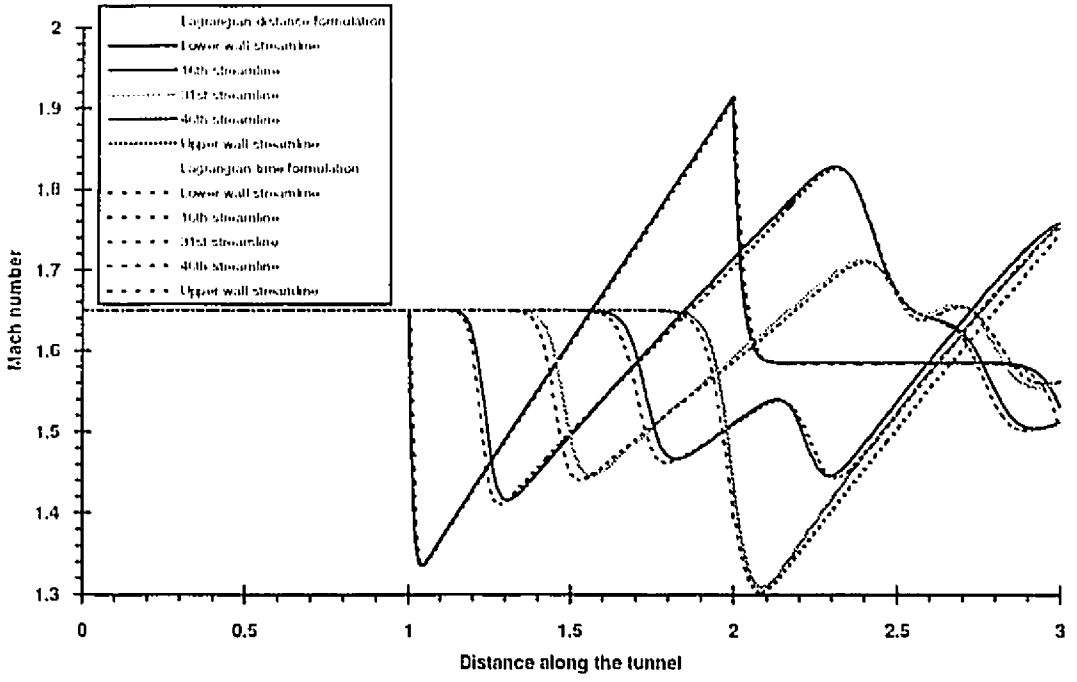

Figure 12. Mach number comparison for Lagrangian-time and distance formulations

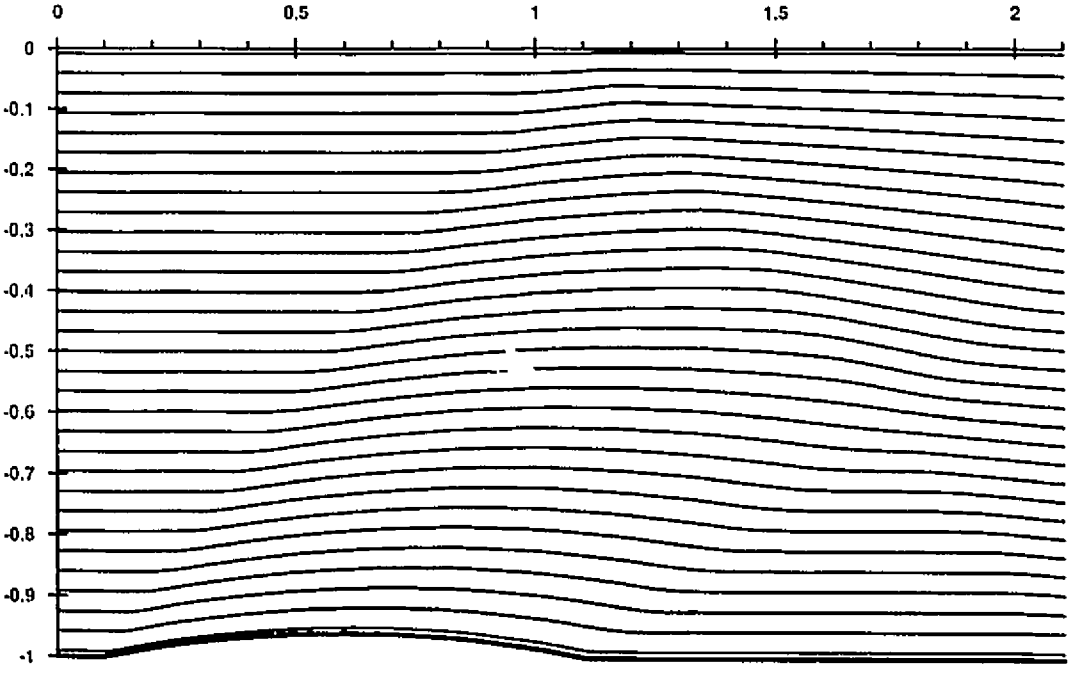

Figure 13. Streamlines and wall shape for the circular arc bump

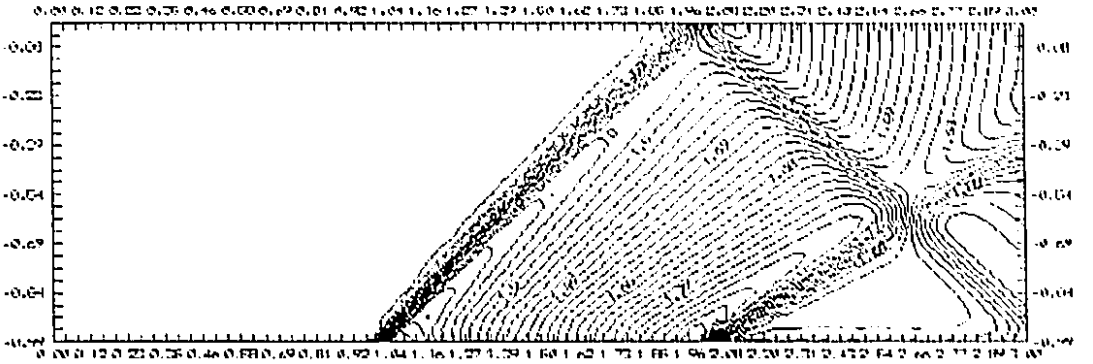

Figure 14. Mach Number isolines for the circular arc bump problem

5.1.2 Flow in a tunnel with a straight wedge

This problem consists of a supersonic flow past a straight wedge as shown in figure 15. The inlet Mach number is 2.0, the wedge angle is 8 Degree, the wedge length is 1 and the tunnel height is 1. The sharp corners involved, where an oblique shock or expansion fan is issued, are treated in the way described in section 5.1.1 to ensure that the shock, and expansion fan, will be issued at a cell corner (see figure 10).

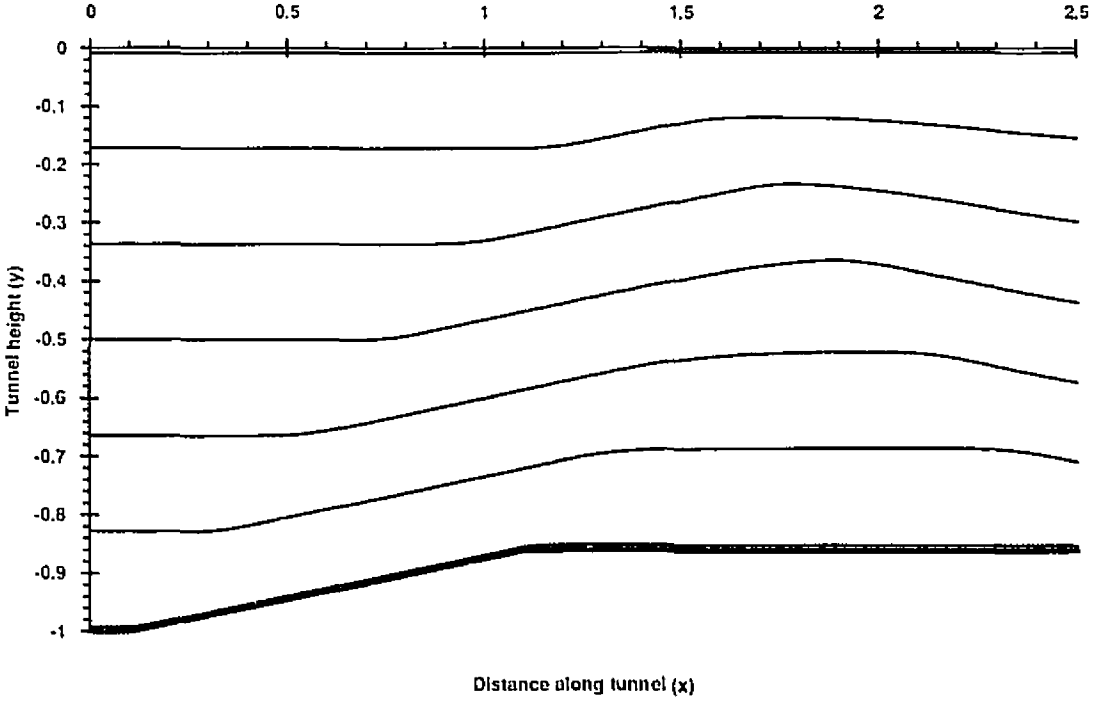

Figure 15. Wall and streamlines shape for the straight wedge problem

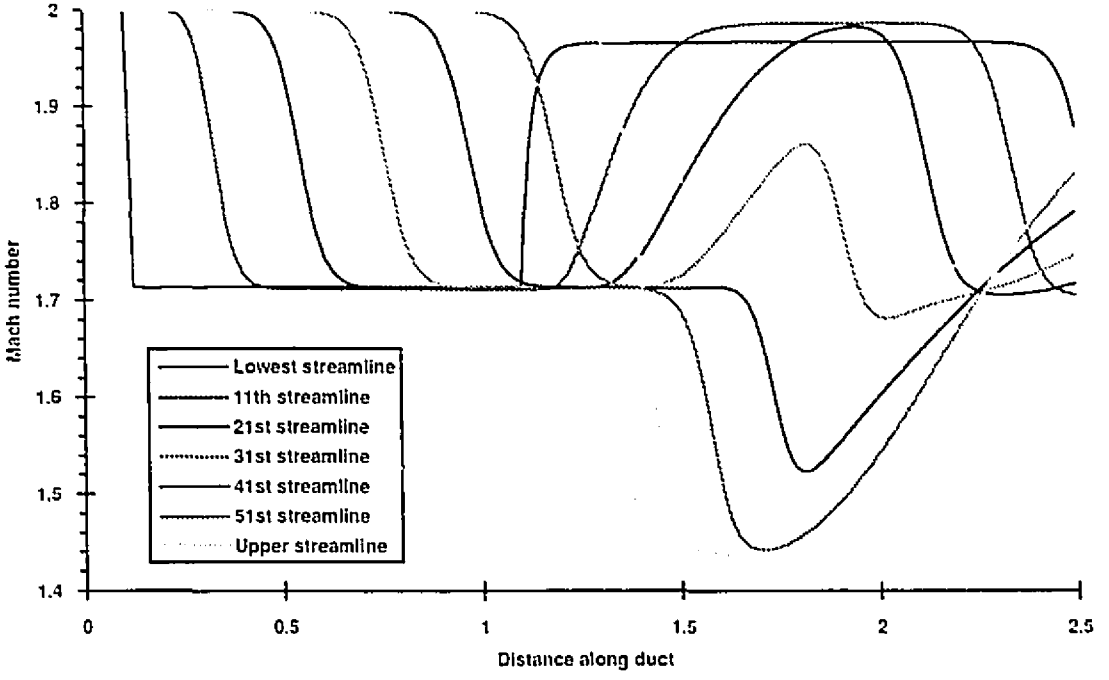

Figure 16. Mach number distribution for the straight wedge problem

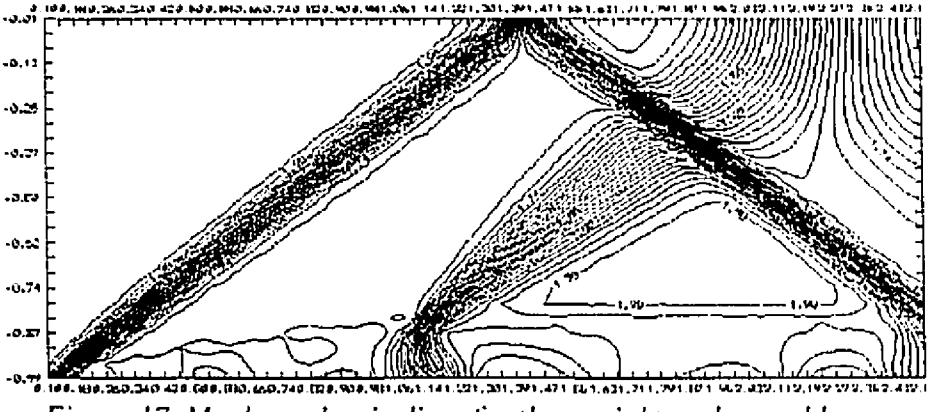

Figure 17. Mach number isolines for the straight wedge problem

5.1.3 Flow through a simple (parabolic) supersonic nozzle

The problem is the case of a simple supersonic nozzle made up of two parabolas smoothly connected. The nozzle wall is build of two parabolas ($y=ax^2+bx+c$). The two parabolas starts each at one end of the nozzle and are connected at the middle (see figure 18). The exit of the nozzle is fitted with an extended straight pipe section to allow for dampening the fluid oscillations at nozzle exit and reach a uniform flow. The nozzle being symmetric about its axis only one half (the lower half) is considered. All the nozzle problems were solved using the Lagrangian formulation based on Lagrangian-distance. The boundaries streamlines are recessed from the wall as described in section 4.6.1. We considered various nozzles with varying lengths and area ratios. We present here the results for three nozzle cases, representing a long, intermediate length and short nozzle. All the three nozzles have the same area ratio. Very short nozzles (or ones with a very high area ratio) develop an inclined shock wave at exit (figures 25, 22 and 24), This is in contrast with the properly designed nozzle of section (figure 35), which exits a uniform flows.

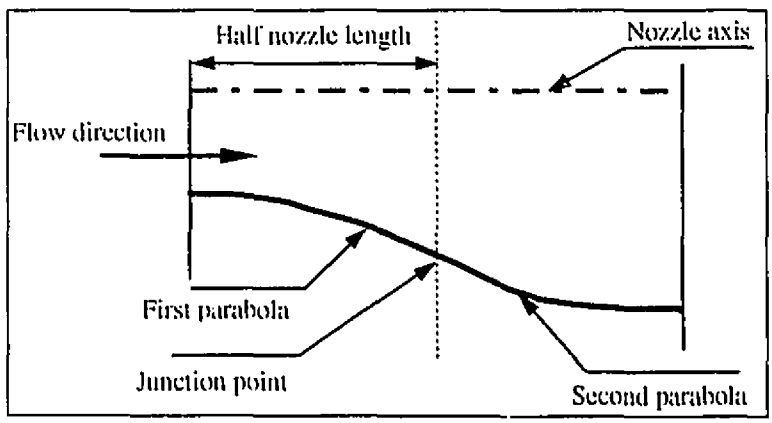

Figure 18. Parabolic nozzle construction

5.1.4 Case of a long nozzle.

This is the application of the nozzle problem described in section 5.1.3 to a relatively long nozzle. The Mach number at inlet to the nozzle is 1.05, the solution is for

15 streamlines, the area ratio is equal to 4 and the inlet are equals 0.5. The nozzle length is 40 with a straight extension of the exit of length 20.

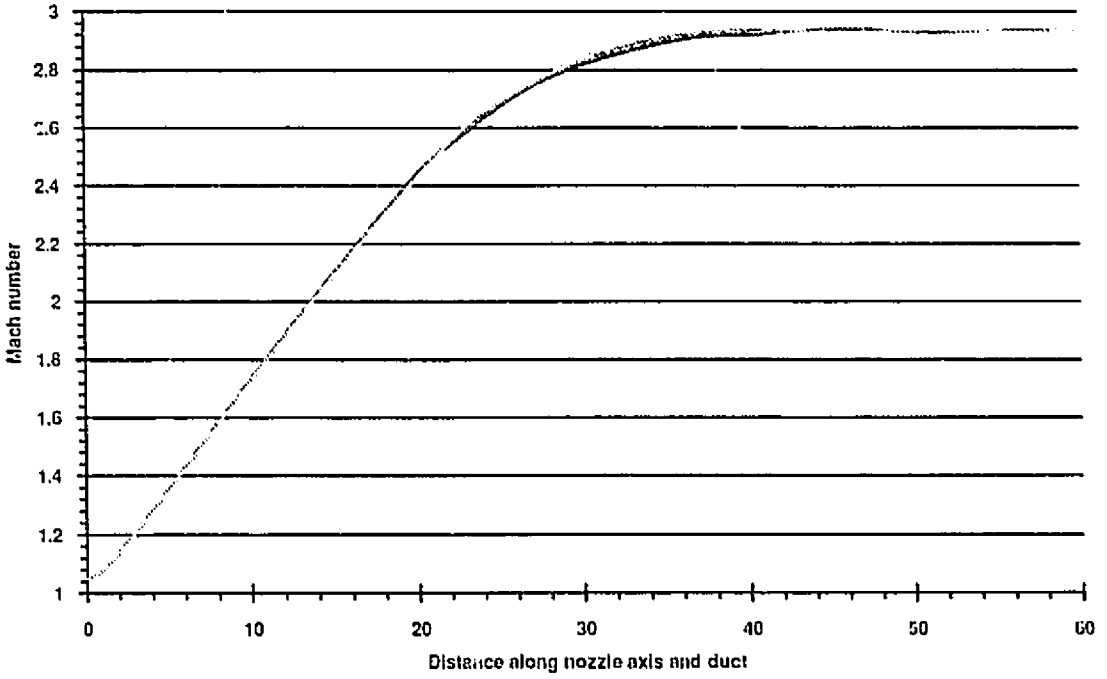

Figure 19. Mach number distribution in a long parabolic nozzle

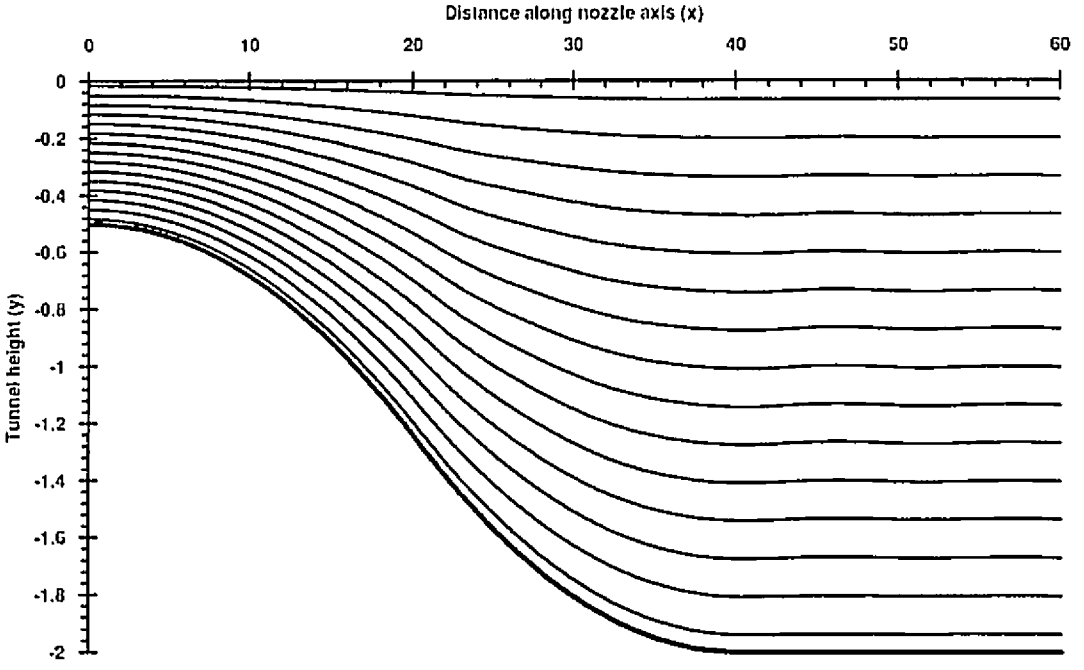

Figure 20. Streamlines and wall shape in a long parabolic nozzle

5.1.5 The case of an intermediate-length nozzle.

This is the application of the nozzle problem described in section 5.1.3 to a intermediate length nozzle. The Mach number at inlet to the nozzle is 1.05, the solution is for 15 streamlines, the area ratio is equal to 4 and the inlet are equals 0.5. The nozzle length is 10 with a straight extension of the exit of length 50. The longer extension to the outlet of the nozzle is intended to observe the oscillations at nozzle exit.

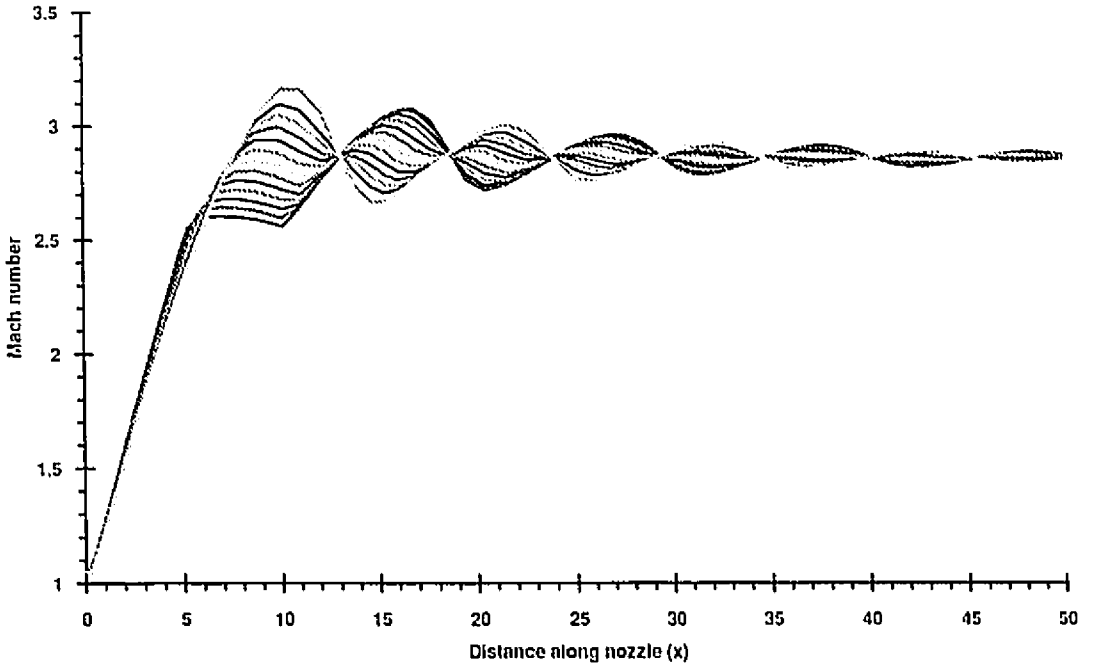

Figure 21. Mach number distribution for an intermediate length parabolic nozzle

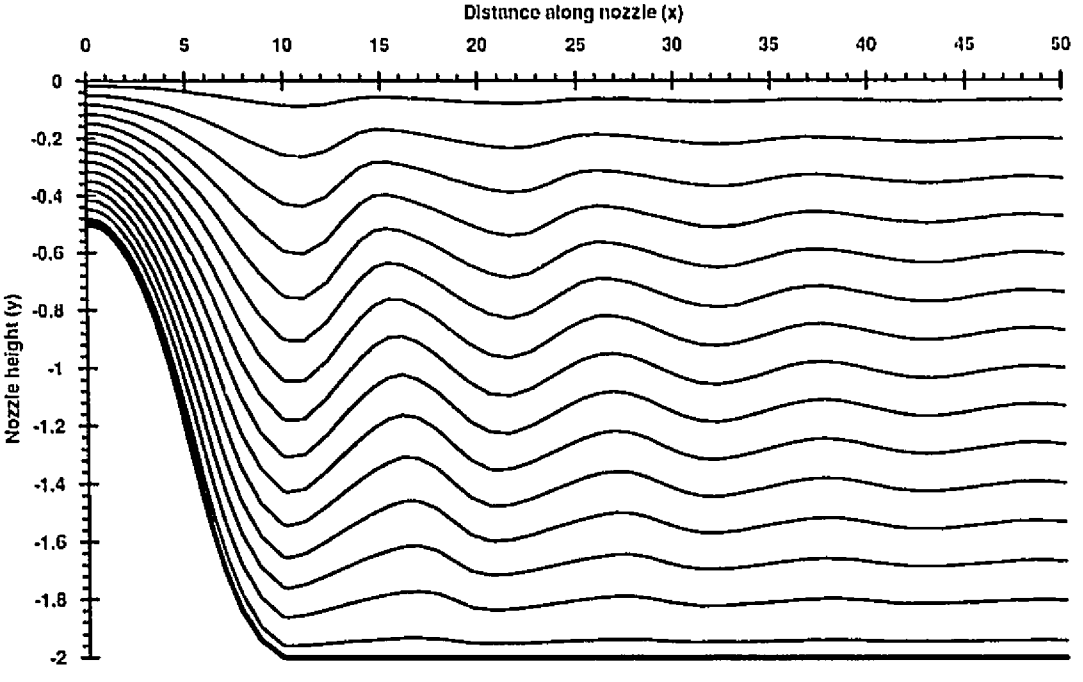

Figure 22. Streamlines and wall shape for an intermediate length parabolic nozzle

5.1.6 Case of a short nozzle.

This is the application of the nozzle problem described in section 5.1.3 to a short nozzle. The Mach number at inlet to the nozzle is 1.05, the solution is for 15 streamlines, the area ratio is equal to 4 and the inlet are equals 0.5. The nozzle length is 3 with a straight extension of the exit of length 60. The longer extension to the outlet of the nozzle is intended to observe the oscillations at nozzle exit.

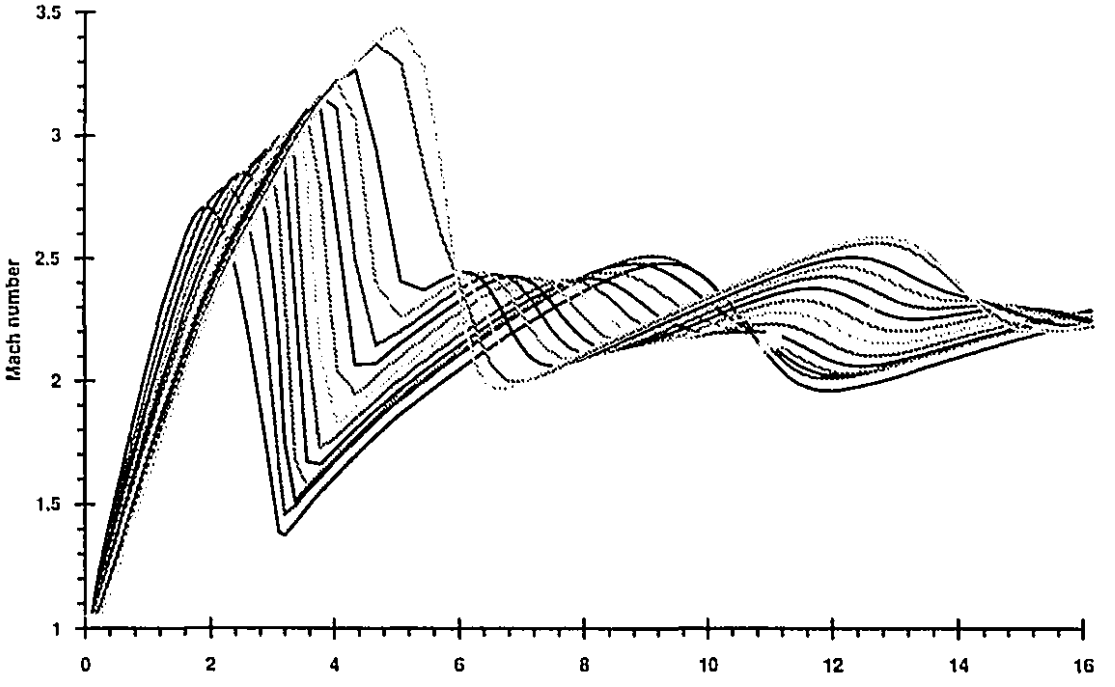

Figure 23. Mach number distribution for a short parabolic nozzle (enlarged inlet)

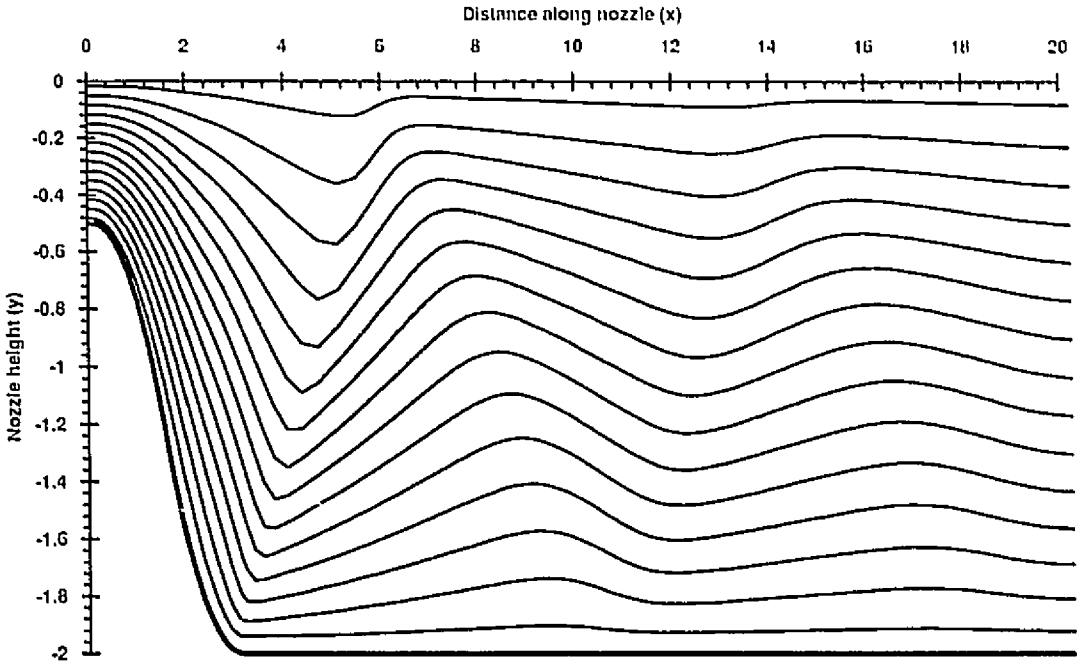

Figure 24. Streamlines and wall shape for the short parabolic nozzle

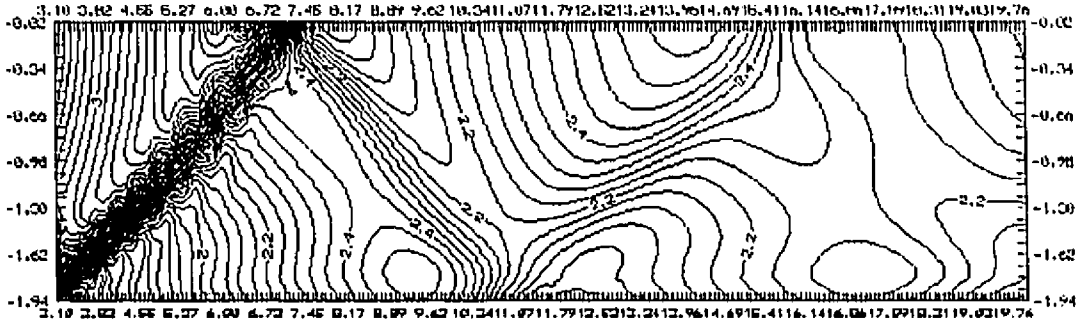

Figure 25. Mach number isolines at the exit of the short parabolic nozzle

5.1.7 Problem of airfoils at incidence

In this problem the flow around an airfoil made up of two circular ares (lenticular airfoil) at incidence is computed. The airfoil problems were solved using the Lagrangian formulation based on Lagrangian-distance. The boundary streamlines are recessed from the wall as described in section 4.6.1. The airfoil is placed in the middle of a duct.

5.1.8 Case of a lenticular airfoil at low supersonic Mach number

The airfoil problem described in section 5.1.7 is first applied to an airfoil submitted to a relatively low Mach number. Figure 28 shows the shape of the airfoil and the two closest streamlines. The figure is enlarged to show the interesting region of the flow. The Mach number is equal to 2.0, the problem is solved for 120 streamlines (60 on each side of the airfoil). The incidence angle is equal to 7 Degree.

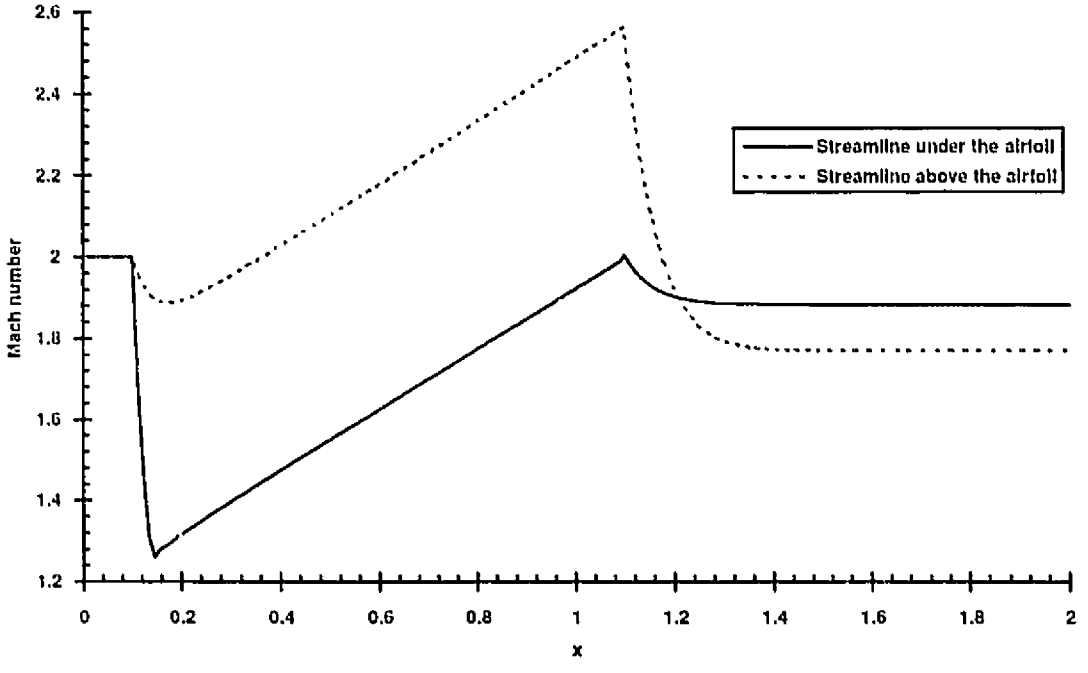

Figure 26. Mach number distribution for the lenticular airfoil at Mach number=2.0

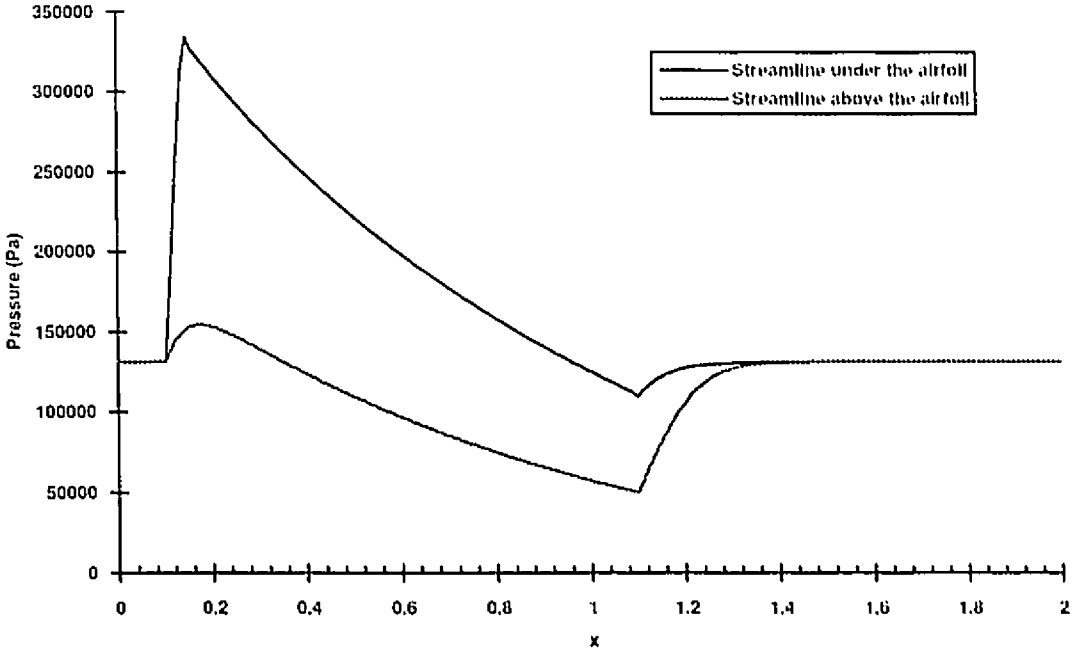

Figure 27. Pressure distribution for the lenticular airfoil at Mach number=2.0

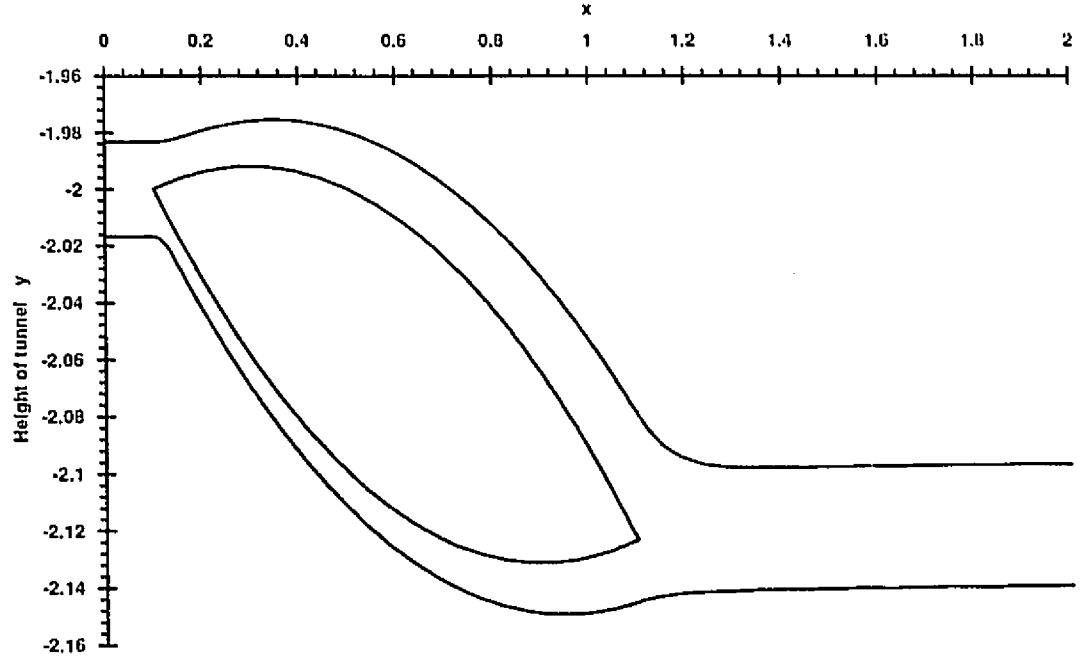

Figure 28. Airfoil and streamline shape for airfoil at Mach number = 2.0

5.1.9 Case of a lenticular airfoil at high Mach number

The airfoil problem described in section 5.1.7 is then applied to an airfoil submitted to a relatively high Mach number. Figure 31 shows the shape of the airfoil and the two closest streamlines. The figure is enlarged to show the interesting region of the flow. The Mach number is equal to 5.0, the problem is solved for 120 streamlines (60 on each side of the airfoil). The incidence angle is equal to 7 Degree.

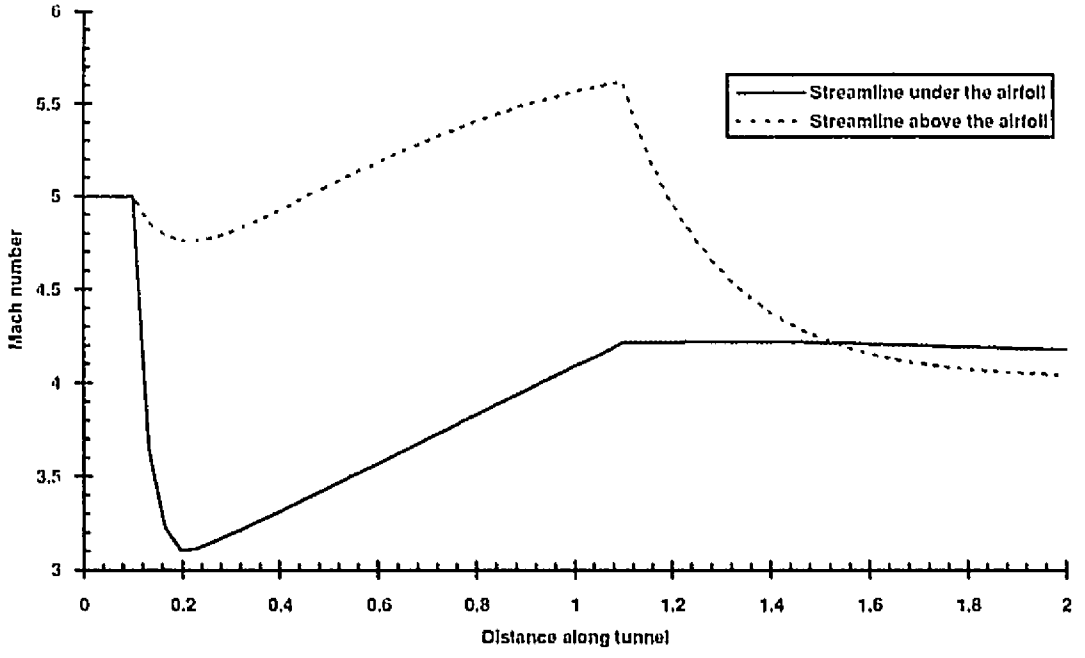

Figure 29. Mach number distribution for lenticular airfoil at Mach number=5.0

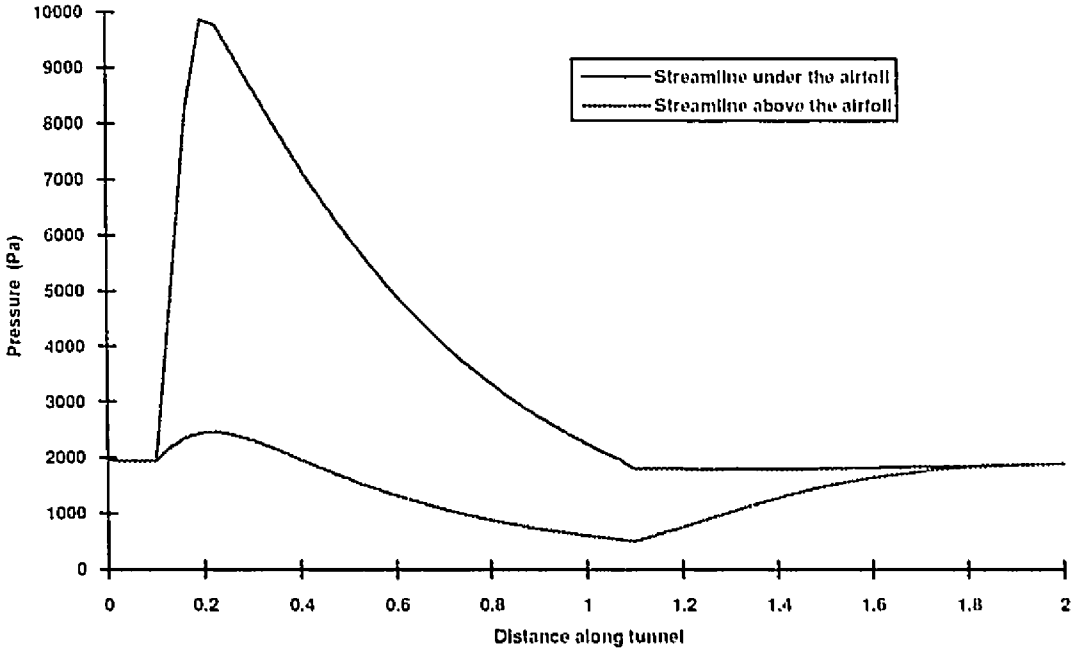

Figure 30. Pressure distribution for lenticular airfoil at Mach number=5.0

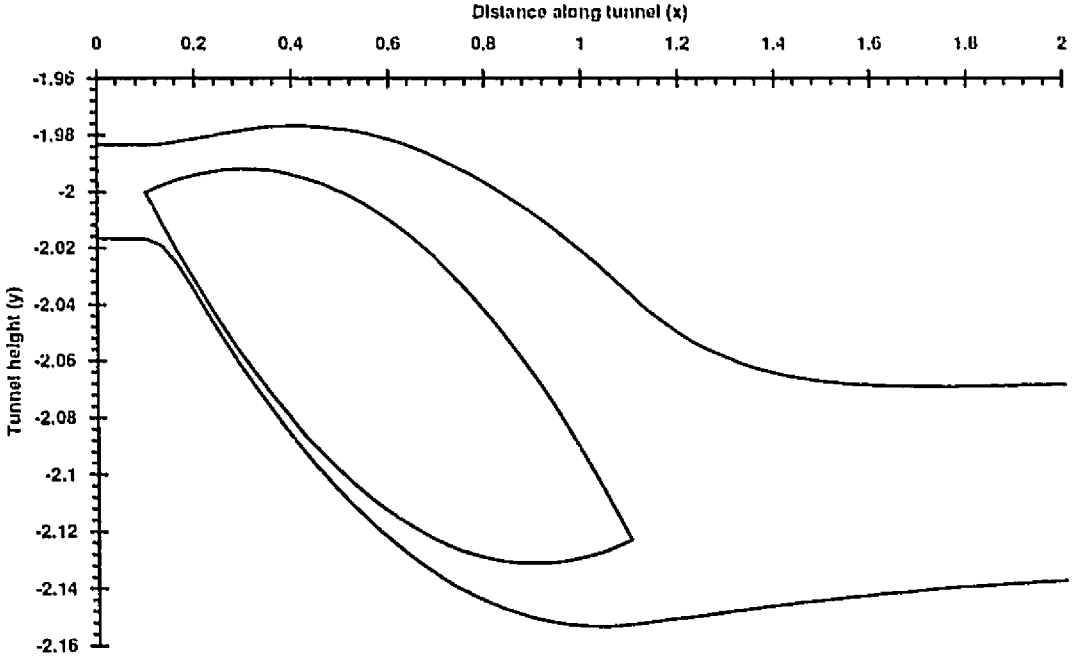

Figure 31. Airfoil and streamlines shape at Mach number=5.0

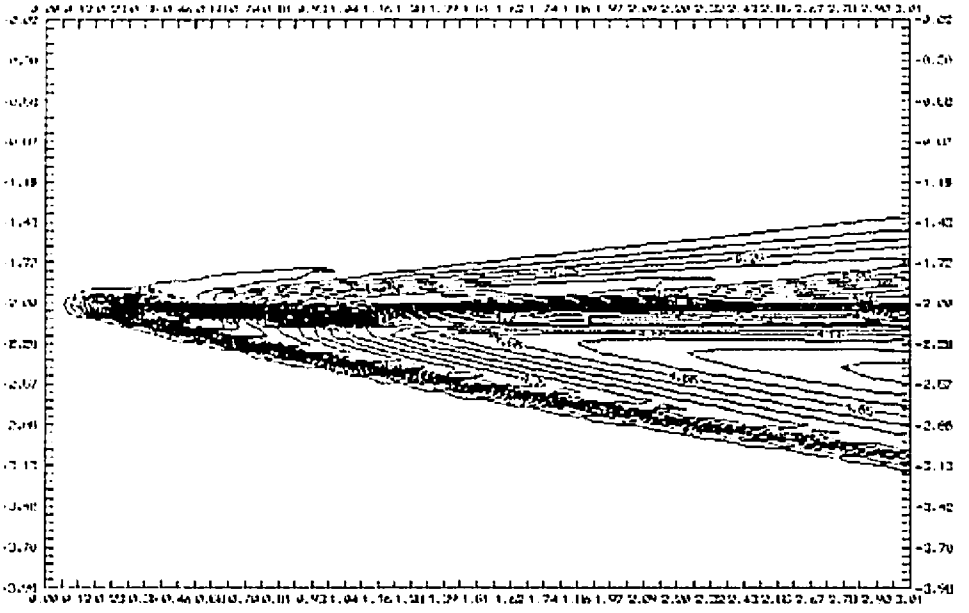

Figure 32. Mach number isolines around the airfoil at Mach number=5.0

5.2 Unspecified geometry problems (shape prediction)

In this problem we consider the possibility to compute the flow around bodies whose shape is not specified, instead we know one condition that restricts the flow and provides for the missing information of the body-shape. We then compute the shape of the body subjected to the flow in such a way that this condition be satisfied. This type of problem were made possible by the fact that the Lagrangian formulation does not require a grid generation [16]. This is opposed to an Euler based representation where a grid is needed and can only be generated if the shape of the body implied is known. Thus it appears that this type of inverse solution (shape computing) is only possible with this kind of Lagrangian based solution. Two specific problems were solved in this case: (i) The case of computing the body shape to produce a required pressure distribution, (ii) and the problem of nozzle design.

5.2.1 Computing the shape of a circular arc to satisfy a given pressure distribution

Here we want to compute the shape of a body that will produce a particular pressure distribution. In order to have a reference to verify the program's output, the pressure distribution was computed on the wall for the circular arc bump problem of section 5.1.1 and fed to the program to compute the shape.

The difference in the procedure to compute the shape appears only when solving for the boundary streamline, and the procedure is similar to that described in section 4.6.1. At any moment $\tau=n\Delta\tau$ (or $\lambda=n\Delta\lambda$) we want to compute the flux at the wall at $j=1/2$ and $n=n+1/2$. We do not now the shape of the wall at but we do now the pressure at $j=1/2$ and $n=n+1/2$.

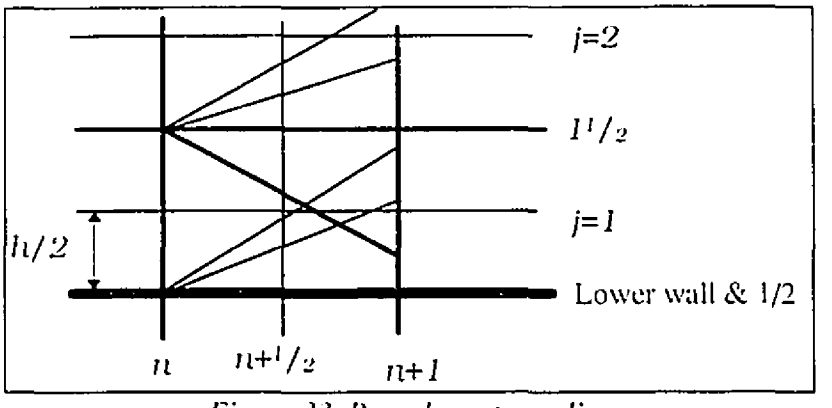

Figure 33. Boundary streamline

$$\alpha = \frac{p_{1/2}^{n+1/2}}{p_1^n}, \tag{5.1}$$

where α is the pressure ratio of the known pressure at $j=1/2$ and $n=n+1/2$ to the pressure at j and n. If a is greater than one we compute the wall direction directly with the Rankine-Hugoniot equation

$$\theta_{1/2}^{n+1/2} = \theta_1^n + \tan^{-1}\left[\frac{\alpha - 1}{\gamma\left(M_1^n\right)^2 - \alpha + 1}\cdot\sqrt{\frac{2\gamma\left(M_1^n\right)^2}{(\gamma+1)\alpha + \gamma - 1} - 1}\right]. \tag{5.2}$$

If α is smaller than one, in the case of an expansion, we first compute the Mach number at $j=1/2$ and $n=n+1/2$ based on the isentropic equation

$$\left(M_{1/2}^{n+1/2}\right)^2 = \frac{2}{\gamma - 1}\left(\frac{1 + \frac{\gamma - 1}{2}\left(M_1^n\right)^2}{\alpha^{\frac{\gamma-1}{\gamma}}} - 1\right), \tag{5.3}$$

and we compute the wall direction using the characteristic relation

$$\theta_{1/2}^{n+1/2} = \theta_1^n + \nu\left(M_1^n\right) - \nu\left(M_{1/2}^{n+1/2}\right), \tag{5.4}$$

where ν is the Prandtl-Meyer expansion function

$$\nu(M) = \sqrt{\frac{\gamma+1}{\gamma-1}}\tan^{-1}\left(\sqrt{\frac{\gamma-1}{\gamma+1}}\sqrt{M^2-1}\right) - \tan^{-1}\sqrt{M^2-1}\,. \tag{5.5}$$

This problem was solved using the Lagrangian formulation based on Lagrangian-distance. The boundaries streamlines are recessed from the wall as described in section 4.6.1. The shape output was then compared to the original shape. The result of this comparison is shown in figure 34. The inlet Mach number is equal to 1.65 and the problem is solved for 60 streamlines.

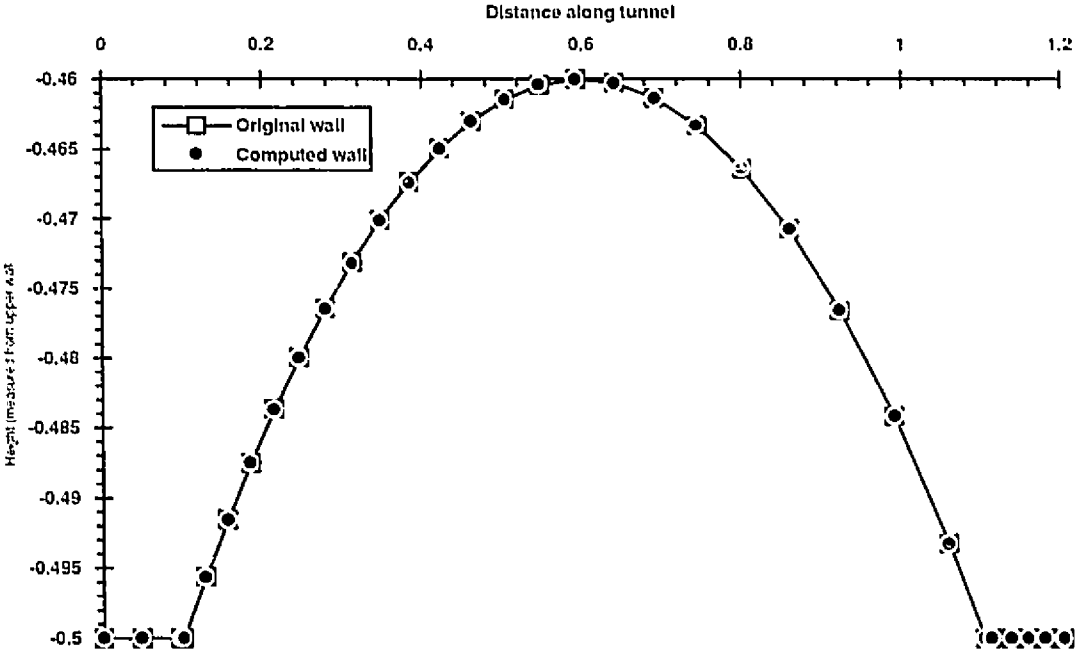

Figure 34. Wall shape comparison

5.2.2 Supersonic nozzle design problem

The ability of the Lagrangian method to solve problems of undetermined initial shape is used to compute the shape of the expansion section of a supersonic nozzle. This idea is similar to the reflection suppression problem described by Anderson [1]. The required condition is that the flow at outlet be uniform. This is achieved by setting the wall shape in such a way that there be no wave reflection from the wall. Numerically this is achieved by setting the wall direction at each step n to be parallel to the direction of the lowest streamline (the streamline that is the closest to the wall) at that step n. Note that this solution is satisfying the reflection suppression condition by forcing the wall to follow the closest streamline's shape. This is effectively a reversed solution, as when the wall shape is known, then the lowest streamline would be following its shape.

This problem was solved using the Lagrangian formulation based on Lagrangian-time. The upper boundary streamline is recessed from the wall as described in section 4.6.1, while the lower streamline is positioned on the lower wall and confined using an image flow as described in section 4.6.2.

A circular arc is set up at inlet to provide for a smooth expansion. This is necessary to avoid a sharp corner expansion at inlet that could cause separation of the flow.

Figure 35 shows the Mach number distribution at the exit of this type of nozzle to be uniform as required.

The Mach number at inlet is set to 1.001, the problem was solved for 201 streamlines, the inlet height was 1 and the computed outlet height was 42.4548.

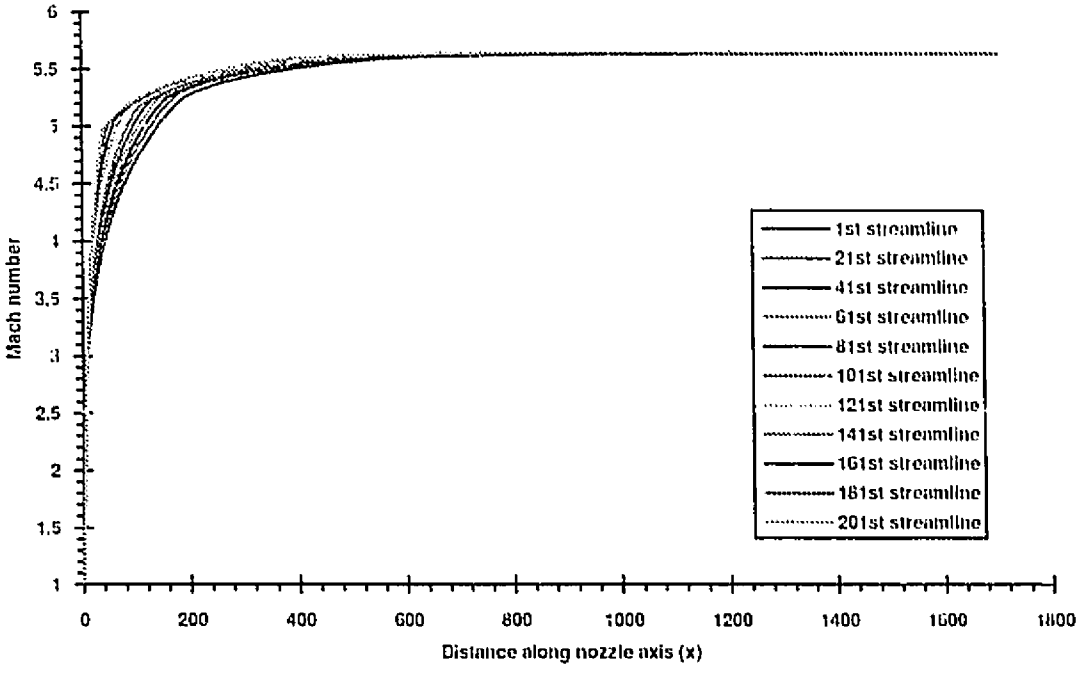

Figure 35. Mach number distribution along the designed nozzle axis

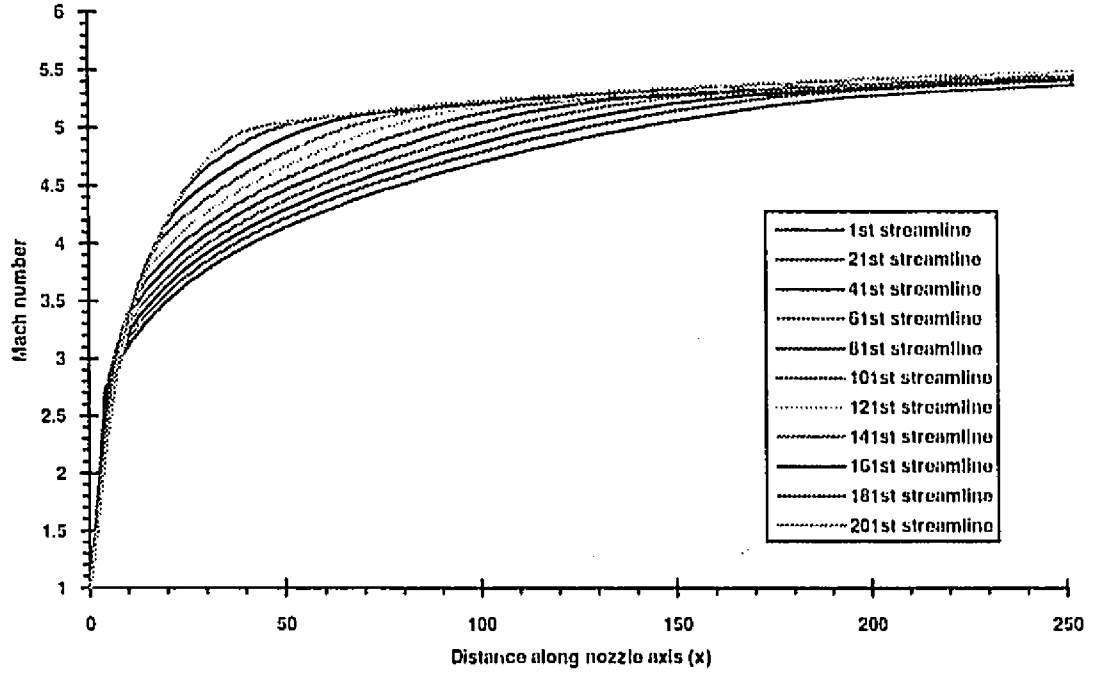

Figure 36. Mach number distribution along the designed nozzle axis (enlarged inlet)

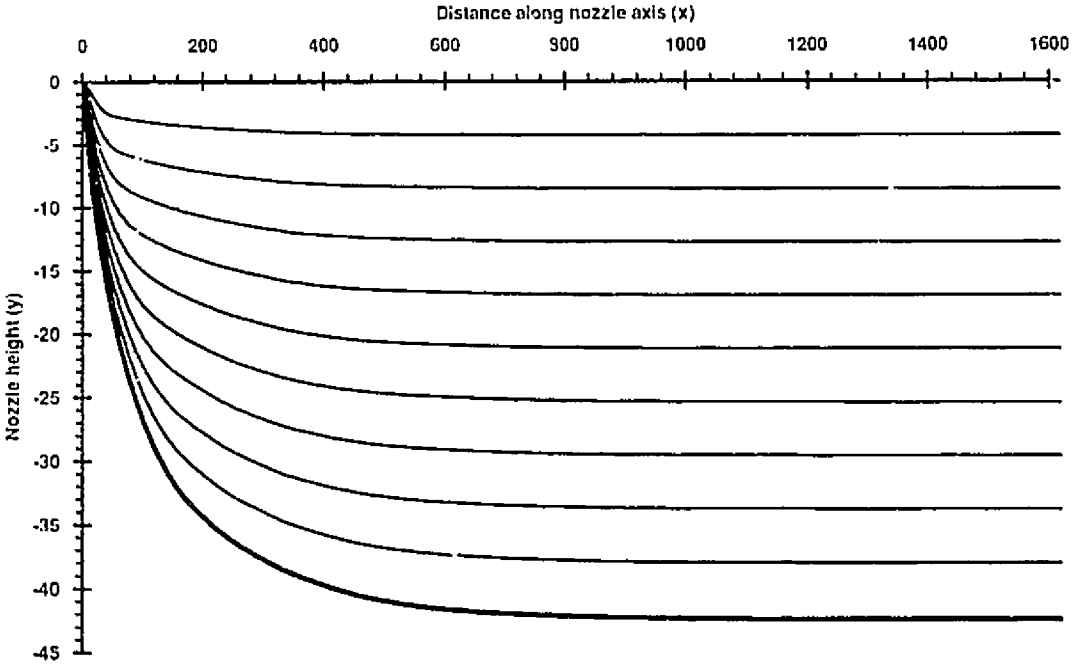

Figure 37. Designed nozzle and streamlines shape

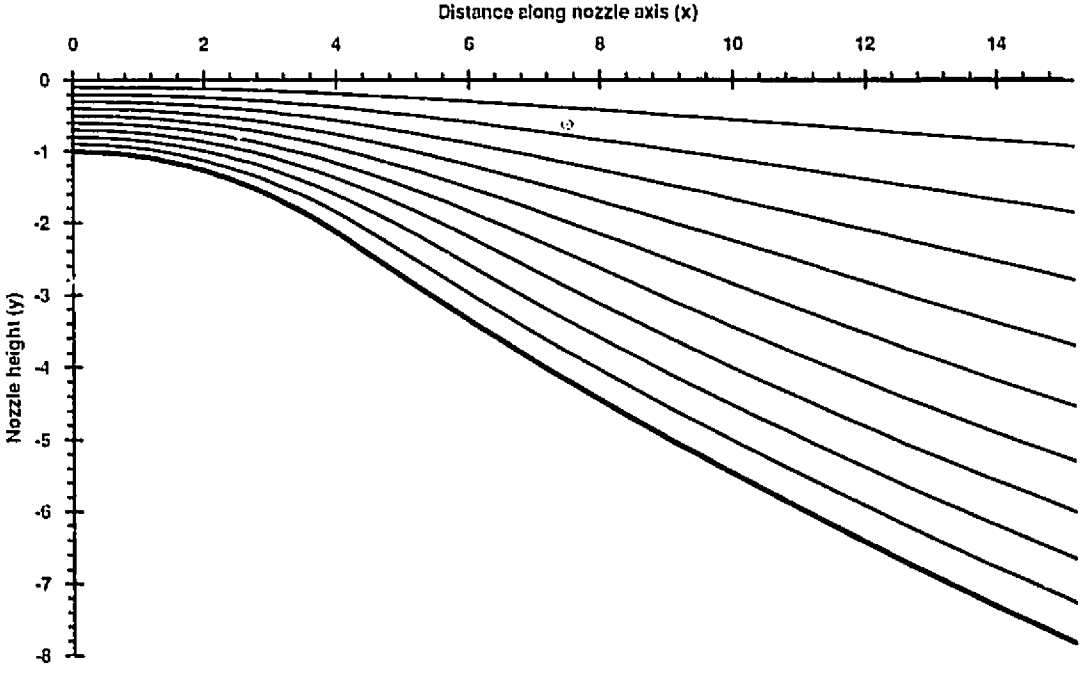

Figure 38. Designed nozzle and streamlines shape (enlarged inlet section)

6. CONCLUSIONS

In the present work we analyzed the capabilities of a Lagrangian formulation of Euler equations of motion introduced by Hui and Loh [11]. Two variants of this formulation were examined: (i) The Lagrangian formulation based on Lagrangian-time, and (ii) the Lagrangian formulation based on Lagrangian-distance.

In the Lagrangian-time formulation fluid particles are followed along their streamlines at their own speed, while the formulation based on Lagrangian-distance retains the property of tracing a fluid particle, but in relation to the distance traveled along the streamline. Numerically, this means that a computational cell using Lagrangian-distance marches in the flow direction of the fluid particle, but not with its real speed.

A numerical scheme was developed to solve the Euler equations of motion using these two Lagrangian formulations and was tested for standard problems, in comparison with results obtained using Eulerian formulation.

Then the ability of the Lagrangian-based formulation to solve aerodynamic problems of unspecified body shape was investigated. Two situations of unknown body-shape were considered:

I. In the first case, we computed the shape of a body that would produce a known (or required) pressure distribution when subjected to a specified flow. The pressure distribution being used as input to the program.

II. The second case studied was the design of a supersonic nozzle. In this case, the reflection suppression condition was used to define the problem, in order to obtain a uniform supersonic flow at the exit.

The solutions obtained with this Lagrangian method were found to be very accurate, displaying a high computational efficiency (actually providing second-order accuracy at a computational load of a first-order solution).

APPENDIX A

The Jacobian of the coordinates transformation

This appendix is intended as a reminder to the relation governing the transformation between two coordinates systems.

Starting from the following relation linking the x - y system to the τ - ξ system:

$$\left.\begin{aligned} d\tau &= \frac{\partial \tau}{\partial x}dx + \frac{\partial \tau}{\partial y}dy \\ d\xi &= \frac{\partial \xi}{\partial x}dx + \frac{\partial \xi}{\partial y}dy \end{aligned}\right\}, \tag{A.1}$$

$$\left.\begin{aligned} dx &= \frac{\partial x}{\partial \tau}d\tau + \frac{\partial x}{\partial \xi}d\xi \\ dy &= \frac{\partial y}{\partial \tau}d\tau + \frac{\partial y}{\partial \xi}d\xi \end{aligned}\right\}, \tag{A.2}$$

which can be written in matrix representation as follows:

referring to equation A.1

$$\begin{vmatrix} d\tau \\ d\xi \end{vmatrix} = \underbrace{\begin{vmatrix} \frac{\partial \tau}{\partial x} & \frac{\partial \tau}{\partial y} \\ \frac{\partial \xi}{\partial x} & \frac{\partial \xi}{\partial y} \end{vmatrix}}_{T^{-1}} \cdot \begin{vmatrix} dx \\ dy \end{vmatrix}, \tag{A.3}$$

and referring to equation (A.2)

$$\begin{vmatrix} dx \\ dy \end{vmatrix} = \underbrace{\begin{vmatrix} \frac{\partial x}{\partial \tau} & \frac{\partial x}{\partial \xi} \\ \frac{\partial y}{\partial \tau} & \frac{\partial y}{\partial \xi} \end{vmatrix}}_{T} \cdot \begin{vmatrix} d\tau \\ d\xi \end{vmatrix}. \tag{A.4}$$

Solving for the determinant of the matrix T^{-1} we get

$$\det\ T^{-1} = \frac{1}{J} = \frac{\partial \tau}{\partial x}\frac{\partial \xi}{\partial y} - \frac{\partial \tau}{\partial y}\frac{\partial \xi}{\partial x}, \tag{A.5}$$

and for T we get

$$\det\ T = J = \frac{\partial x}{\partial \tau}\frac{\partial y}{\partial \xi} - \frac{\partial x}{\partial \xi}\frac{\partial y}{\partial \tau}, \tag{A.6}$$

where J is the determinant of the transformation and called the **Jacobian.**

From equation (A.2) we get:

$$d\xi = \frac{dx - \left(\partial x / \partial \tau\right) d\tau}{\partial x / \partial \xi}, \tag{A.7}$$

$$dy = \frac{\partial y}{\partial \tau} d\tau + \frac{\partial y}{\partial \xi}\left(\frac{dx - \left(\partial x / \partial \tau\right) d\tau}{\partial x / \partial \xi} \right), \tag{A.8}$$

simplifying we get

$$d\tau = \frac{1}{J}\left(\frac{\partial y}{\partial \xi} dx - \frac{\partial x}{\partial \xi} dy \right), \tag{A.9}$$

and for y constant *(dy=0)* we get:

$$\frac{\partial \tau}{\partial x} = \frac{1}{J}\frac{\partial y}{\partial \xi}, \tag{A.10}$$

while for x constant *(dx=0)* we get:

$$\frac{\partial \tau}{\partial y} = -\frac{1}{J}\frac{\partial x}{\partial \xi} . \tag{A.11}$$

From equation (A.2) we get:

$$d\tau = \frac{dx - \left(\partial x / \partial \xi\right) d\xi}{\partial x / \partial \tau} , \tag{A.12}$$

$$dy = \frac{\partial y}{\partial \tau}\left(\frac{dx - \left(\partial x / \partial \xi\right) d\xi}{\partial x / \partial \tau} \right) + \frac{\partial y}{\partial \xi} d\xi , \tag{A.13}$$

simplifying we get

$$d\xi = \frac{1}{J}\left(\frac{\partial x}{\partial \tau} dy - \frac{\partial y}{\partial \tau} dx \right) , \tag{A.14}$$

and for y constant *(dy=0)* we get:

$$\frac{\partial \xi}{\partial x} = -\frac{1}{J}\frac{\partial y}{\partial \tau} , \tag{A.15}$$

while for x constant *(dx=0)* we get :

$$\frac{\partial \xi}{\partial y} = \frac{1}{J}\frac{\partial x}{\partial \tau} . \tag{A.16}$$

From equation (A.1) we get:

$$dx = \frac{d\tau - \left(\partial \tau / \partial y\right) dy}{\partial \tau / \partial x} , \tag{A.17}$$

$$d\xi = \frac{\partial \xi}{\partial x}\left(\frac{d\tau - \left(\partial\tau/\partial y\right)d\tau}{\partial\tau/\partial x} \right) + \frac{\partial \xi}{\partial y} dy \,. \tag{A.18}$$

simplifying we get

$$dy = J\left(\frac{\partial \tau}{\partial x} d\xi - \frac{\partial \xi}{\partial x} d\tau \right), \tag{A.19}$$

and for ξ constant ($d\xi$=0) we get:

$$\frac{\partial y}{\partial \tau} = -J \frac{\partial \xi}{\partial x} \,, \tag{A.20}$$

while for τ constant ($d\tau$=0) we get :

$$\frac{\partial y}{\partial \xi} = J \frac{\partial \tau}{\partial x} \,. \tag{A.21}$$

From equation (A.1) we get:

$$dy = \frac{d\tau - \left(\partial\tau/\partial x\right)dx}{\partial\tau/\partial y} \,, \tag{A.22}$$

$$d\xi = \frac{\partial \xi}{\partial x} dx + \frac{\partial \xi}{\partial y}\left(\frac{d\tau - \left(\partial\tau/\partial x\right)dx}{\partial\tau/\partial y} \right), \tag{A.23}$$

simplifying we get

$$dx = J\left(\frac{\partial \xi}{\partial y} d\tau - \frac{\partial \tau}{\partial y} d\xi \right), \tag{A.24}$$

and for τ constant ($d\tau$=0) we get:

$$\frac{\partial x}{\partial \xi} = -J \frac{\partial \tau}{\partial y} , \tag{A.25}$$

while for ξ constant ($d\xi$=0) we get:

$$\frac{\partial x}{\partial \tau} = J \frac{\partial \xi}{\partial y} . \tag{A.26}$$

APPENDIX B

The method of characteristics

The method outlined in this appendix is based on the assumption that the fluid is a perfect gas, that the flow is steady, two dimensional, irrotational and isentropic. The preceding condition (assumption) is expressed mathematically by the differential equation of the velocity potential:

$$\left(a^2 - \Phi_x^2\right)\Phi_{xx} - 2\Phi_x\Phi_y\Phi_{xy} + \left(a^2 - \Phi_y^2\right)\Phi_{yy} = 0 \,, \tag{B.1}$$

where

$$\begin{aligned} \Phi_x &= \frac{\partial \Phi}{\partial x} = u; \qquad \Phi_y = \frac{\partial \Phi}{\partial y} = v \\ \Phi_{xx} &= \frac{\partial^2 \Phi}{\partial x^2}; \qquad \Phi_{yy} = \frac{\partial^2 \Phi}{\partial y^2} \\ \Phi_{xy} &= \frac{\partial}{\partial x}\frac{\partial \Phi}{\partial y} \end{aligned} \tag{B.2}$$

u and v are respectively the x and y components of the velocity vector,

Φ is the velocity potential and a is the local speed of sound.

Equation (B.1) is in fact a differential equation of the general type:

$$A\,\Phi_{xx} + 2B\,\Phi_{xy} + C\,\Phi_{yy} = D \,, \tag{B.3}$$

where the coefficient A, B, C and D are functions of x, y, u and v.

Equation (B.1) accepts a solution of the general form:

$$\left(\frac{dy}{dx}\right)_{I,II} = \frac{-\frac{uv}{a^2} \pm \sqrt{\frac{u^2+v^2}{a^2} - 1}}{1 - \frac{u^2}{a^2}} \,, \tag{B.4}$$

and

$$\left(\frac{dv}{du}\right)_{I,II} = \frac{\frac{uv}{a^2} \mp \sqrt{\frac{u^2+v^2}{a^2} - 1}}{1 - \frac{v^2}{a^2}} . \tag{B.5}$$

Equation (B.4) defines two characteristic directions at each point in the physical plane. These directions give the slopes of the physical characteristics at each point. It is evident that this characteristic curves exist only for supersonic flow, when the term under the root is positive, i.e.:

$$u^2 + v^2 > a^2 \quad \text{or} \quad V^2 > a^2 , \tag{B.6}$$

rearranging and simplifying the characteristic equation (B.4), and introducing the notation:

$$\begin{aligned} &u = V\cos\theta; \quad v = V\sin\theta \\ &M = \frac{1}{\sin\mu}; \quad \sqrt{M^2 - 1} = \frac{1}{\tan\mu} \end{aligned} , \tag{B.7}$$

$$\frac{u^2+v^2}{a^2} = \frac{V^2}{a^2} = M^2 = \frac{1}{\sin^2\mu} , \tag{B.8}$$

where θ is the angle of the velocity vector V and μ is the Mach angle, we get:

$$\begin{aligned} \left(\frac{dy}{dx}\right)_I &= \tan(\theta - \mu) = C^- \\ \left(\frac{dy}{dx}\right)_{II} &= \tan(\theta + \mu) = C^+ \end{aligned} \tag{B.9}$$

Equation set (B.9) shows that each of the physical characteristics is inclined at the Mach angle (μ) to the velocity vector, and that the streamline direction at a point in the physical plane bisects the characteristic directions at that point.

B.1 Two dimensional flow with expansion.

Applying the system of continuity, momentum and energy equations between two points of a two dimensional gas flow undergoing an isentropic expansion, we get the following relation between the variation of the Mach number and the flow deflection:

$$d\theta = -\frac{\sqrt{M^2-1}}{1+\frac{\gamma-1}{2}M^2}\frac{dM}{M} = d\nu(M)\ , \tag{B.10}$$

where ν is the Prandtl-Meyer expansion function

$$\nu(M) = \sqrt{\frac{\gamma+1}{\gamma-1}}\tan^{-1}\left(\sqrt{\frac{\gamma-1}{\gamma+1}}\sqrt{M^2-1}\right) - \tan^{-1}\sqrt{M^2-1}\ . \tag{B.11}$$

Integrating we get the following form:

$$\begin{aligned} Q^+ &= \theta + \nu(M) \\ Q^- &= \theta - \nu(M) \end{aligned} \tag{B.12}$$

Equation set (B.12) represents the characteristic value of a flow which is constant along the lines defined by equation set (B.9). That is Q+ is constant along C+, and Q- is constant along C-. Using the two sets of equations together, it is possible to solve for any unknown point in the flow, relating it to two other points where the flow is known. One of the two known points being related to the unknown point through the positive characteristic (Q+), and the other through the negative characteristic (Q-). We get the following relations:

Along the + characteristics

$$\theta_2 = \theta_1 - \nu(M_1) + \nu(M_2)\ , \tag{B.13}$$

and along the - characteristics

$$\theta_2 = \theta_1 + \nu(M_1) - \nu(M_2)\ . \tag{B.14}$$

APPENDIX C

Oblique shock relations

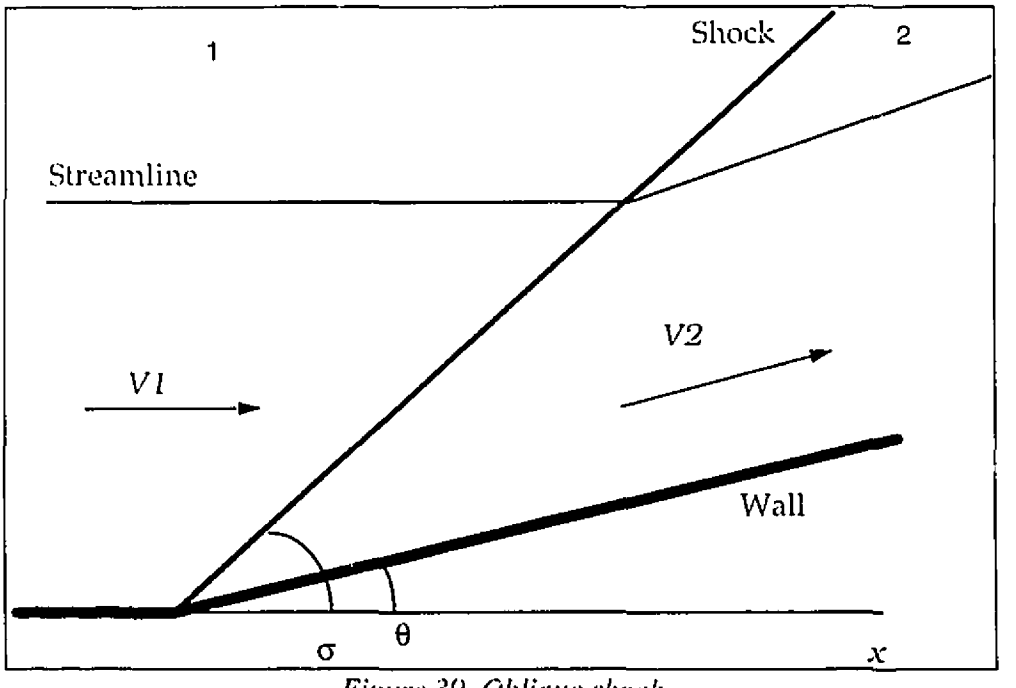

Figure 39. Oblique shock

We analyze the situation represented in figure 39 by writing the continuity, momentum and energy equations for the flow crossing the shock wave situation shown as follows:

C.1 Continuity equation

$$\rho_1 V_{n1} = \rho_2 V_{n2} \tag{C.1}$$

C.2 Momentum equation

Tangent to the shock

$$\begin{aligned}(\rho_1 V_{n1})V_{t1} &= (\rho_2 V_{n2})V_{t2} \\ V_{t1} &= V_{t2} = V_t\end{aligned} \quad , \tag{C.2}$$

and normal to the shock

$$p_1 - p_2 = \rho_2 V_{n2}^2 - \rho_1 V_{n1}^2 \ . \tag{C.3}$$

C.3 Energy equation

$$c_p(T_1 - T_2) = \left(\frac{V_2^2 - V_1^2}{2}\right) . \tag{C.4}$$

were The subscript refer to the following situation (see figure 40)

1	before the shock
2	after the shock
n	normal to the shock
t	tangential to the shock

The fact that the tangential component of velocity does not change across the shock (see equation C.2) and the trigonometry of the velocity triangles (figure 40) lead us to the following result:

$$V_2^2 - V_1^2 = V_{n2}^2 - V_{n1}^2 \ , \tag{C.5}$$

from the perfect gas relation we get:

$$c_p T = c_p\left(\frac{p}{\rho R}\right) = \left(\frac{\gamma}{\gamma - 1}\right)\left(\frac{p}{\rho}\right) , \tag{C.6}$$

The energy equation then becomes:

$$\frac{\gamma}{\gamma - 1}\left(\frac{p_2}{\rho_2} - \frac{p_1}{\rho_1}\right) = \frac{V_{n1}^2 - V_{n2}^2}{2} \ . \tag{C.7}$$

C.4 The Rankine-Hugoniot relations

By eliminating all velocity terms from the basic equations we get a relation between the pressures and densities ratios on both sides of the shock. Rearranging equation (C.3) and using equation (C.1) we get:

$$p_2 - p_1 = \rho_1 V_{n1}^2 \left(1 - \frac{\rho_1}{\rho_2} \right), \tag{C.8}$$

rearranging we get:

$$V_{n1}^2 = \frac{p_2 - p_1}{\rho_2 - \rho_1} \frac{\rho_2}{\rho_1}, \tag{C.9}$$

or equivalently solving for V_{n2} we get:

$$V_{n2}^2 = \frac{p_2 - p_1}{\rho_2 - \rho_1} \frac{\rho_1}{\rho_2}. \tag{C.10}$$

Multiplying (C.9) by (C.10) and simplifying we get:

$$V_{n1} V_{n2} = \frac{p_2 - p_1}{\rho_2 - \rho_1}, \tag{C.11}$$

rearranging and substituting into equation (C.7), we get:

$$\frac{\rho_2}{\rho_1} = \frac{(\gamma + 1)\alpha + \gamma - 1}{\gamma + 1 + (\gamma - 1)\alpha} = \frac{1}{\lambda}, \tag{C.12}$$

where

$$\alpha = \frac{p_2}{p_1}. \tag{C.13}$$

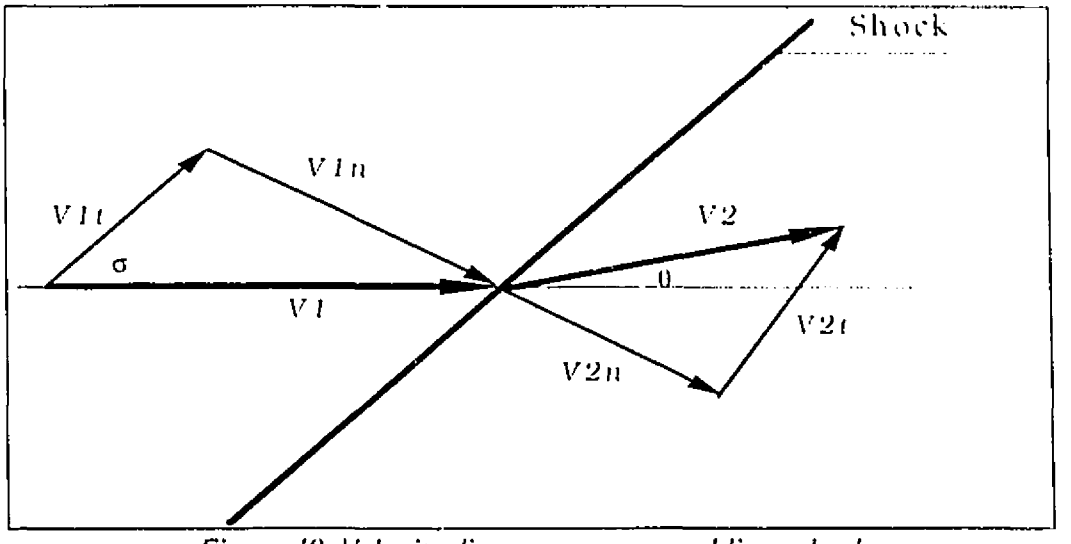

Figure 40. Velocity diagram across an oblique shock

Referring to the geometry of figure 39 and 40 we can write the following relations:

$$V_{t1} = V_1 \cos\sigma$$
$$V_{t2} = V_2 \cos(\sigma - \theta) \quad \text{(C.14)}$$

$$V_{n1} = V_1 \sin\sigma$$
$$V_{n2} = V_2 \sin(\sigma - \theta) \quad \text{(C.15)}$$

$$\frac{V_1}{V_2} = \frac{\cos(\sigma - \theta)}{\cos\sigma} . \quad \text{(C.16)}$$

Rearranging equations (C.1), (C.3) and (C.15) we get:

$$\frac{p_2}{p_1} = 1 + \gamma M_1^2 \sin^2\sigma\left(1 - \frac{\rho_1}{\rho_2}\right) = \alpha , \quad \text{(C.17)}$$

replacing from equation (C.12) we get:

$$\sigma = \sin^{-1}\sqrt{\frac{(\gamma+1)\alpha + \gamma - 1}{2\gamma M_1^2}} , \quad \text{(C.18)}$$

and referring to the geometry of figure 39 we can write the following relations:

$$\tan(\sigma-\theta)=\frac{1}{\lambda}\tan\sigma\ , \tag{C.19}$$

and

$$\frac{1}{\tan\theta}=\left(\frac{\gamma+1}{2}\frac{M_1^2}{M_1^2\sin^2\sigma-1}-1\right)\tan\sigma\ . \tag{C.20}$$

By combining the relations (C.12), (C.17) and (C.18) we get after simplifying:

$$\theta=\tan^{-1}\left[\frac{\alpha-1}{\gamma M_1^2-\alpha+1}\cdot\sqrt{\frac{2\gamma M_1^2}{(\gamma+1)\alpha+\gamma-1}-1}\right], \tag{C.21}$$

where θ is the flow deflection angle after the shock.

The Mach number is defined as the ratio of the local speed to the local speed of sound or:

$$M=\frac{V}{a}=\frac{V}{\sqrt{\gamma RT}}=\frac{V}{\sqrt{\gamma\dfrac{p}{\rho}}}\ , \tag{C.22}$$

$$M^2=\frac{V^2\rho}{\gamma P}\ . \tag{C.23}$$

$$\frac{M_2^2}{M_1^2}=\frac{V_2^2\rho_2}{\gamma p_2}\cdot\frac{\gamma p_1}{V_1^2\rho_1}=\frac{V_2^2}{V_1^2}\cdot\frac{p_1}{p_2}\cdot\frac{\rho_2}{\rho_1}\ . \tag{C.24}$$

Combining equations (C.12), (C.15), (C.14) and (C.24) we get:

$$M_2=\sqrt{\frac{M_1^2\{(\gamma+1)\alpha+\gamma-1\}-2(\alpha^2-1)}{\alpha\{(\gamma-1)\alpha+\gamma+1\}}}\ , \tag{C.25}$$

equation (C.25) expresses the Mach number after the shock as a function of the pressure ratio α and the Mach number before the shock.

APPENDIX D

Solving for the properties of the fluid

At every point during the solution process a complete set of relations (e_1 to e_6) representing the fluid flow at the next time step is computed according to equation (4.11). This relations have the following representation:

$$e_1 = K = \rho(uV - vU) \tag{D.1}$$

$$e_2 = H = \frac{(u^2 + v^2)}{2} + \frac{\gamma}{\gamma - 1}\frac{p}{\rho} \tag{D.2}$$

$$e_3 = Ku + pV \tag{D.3}$$

$$e_4 = Kv - pU \tag{D.4}$$

$$e_5 = U \tag{D.5}$$

$$e_6 = V \tag{D.6}$$

From these preceding relations we now want to compute the actual flow properties.

We start by combining equations (D.5), (D.4) and (D.1), we get:

$$v = \frac{e_4 + pe_5}{K} \tag{D.7}$$

And combining equations (D.6), (D.3) and (D.1) we get:

$$u = \frac{e_3 - pe_6}{K} \tag{D.8}$$

Combining equations (D.7) and (D.8) in (D.2) we get:

$$e_2 = H = \frac{1}{2}\left(\frac{(e_3 - pe_6)^2}{K^2} + \frac{(e_4 + pe_5)^2}{K^2}\right) + \frac{\gamma}{\gamma - 1}\frac{p}{\rho} \tag{D.9}$$

Combining equations (D.7) and (D.8) in (D.1) we get:

$$K^2 = \rho\left(e_3 e_6 - pe_6^2 - e_4 e_5 - pe_5^2\right) \tag{D.10}$$

Combining D.9 and D.10 and simplifying we get:

$$0 = -p^2\left(e_6^2 + e_5^2\right)\frac{\gamma + 1}{2(\gamma - 1)} + p\frac{1}{\gamma - 1}(e_3 e_6 - e_4 e_5) + \frac{\left(e_3^2 + e_4^2\right)}{2} - K^2 H \tag{D.11}$$

Equation (D.11) is a quadratic equation in term of p and can be solved to compute the pressure.

We start by setting:

$$A = -\left(e_6^2 + e_5^2\right)\frac{\gamma + 1}{2(\gamma - 1)} \tag{D.12}$$

$$B = \frac{1}{\gamma - 1}(e_3 e_6 - e_4 e_5) \tag{D.13}$$

$$C = \frac{\left(e_3^2 + e_4^2\right)}{2} - K^2 H \tag{D.14}$$

$$p = \frac{-B + \sqrt{B^2 - 4AC}}{2A} \tag{D.15}$$

Having computed p we can compute the remaining properties by substituting backward into equation (D.7) and (D.8) to get u and v, then in (D.1) to get ρ.

APPENDIX E

Isentropic relations

This appendix is a simple review of the basic relations that exist between the properties of a gas undergoing an isentropic process.

For a gas (compressible fluid) flowing at Mach number M, the ratio of the static pressure p to the stagnation pressure can be written as follows:

$$\frac{p_0}{p} = \left(1 + \frac{\gamma - 1}{2} M^2\right)^{\frac{\gamma}{\gamma-1}} \tag{E.1}$$

Assuming that the stagnation pressure is constant throughout an isentropic shockless flow, we can relate two states of the flow as follows:

$$M_2^2 = \frac{2}{\gamma - 1}\left(\frac{1 + \frac{\gamma - 1}{2} M_1^2}{\alpha^{\frac{\gamma-1}{\gamma}}} - 1\right) \tag{E.2}$$

Where:

$$\alpha = \frac{p_2}{p_1} \tag{E.3}$$

It is also possible to get the ratio of the densities as follows:

$$\frac{\rho_2}{\rho_1} = \alpha^{\frac{1}{\gamma}} \tag{E.4}$$

Knowing the Mach number, pressure and density at any state it is possible to compute the velocity as follows:

$$V = M\sqrt{\frac{\gamma p}{\rho}} \tag{E.5}$$

$$\begin{aligned} u &= V\cos\theta \\ v &= V\sin\theta \end{aligned} \tag{E.6}$$

where the subscripts 1 and 2 refer to two states of the flow, and θ is the flow direction angle.

APPENDIX F

The stability condition

The solution developed in this work is based on a numerical discretization of the Euler equation of motion. This type of solution is bound to instabilities unless special care is taken to prevent them. This is done through the introduction of a stability condition in the solution which states that the domain of numerical dependence must not exceed the domain of physical dependence for the system to be stable, which is expressed in terms of the Courant-Friedrich-Levy number (in short CFL).

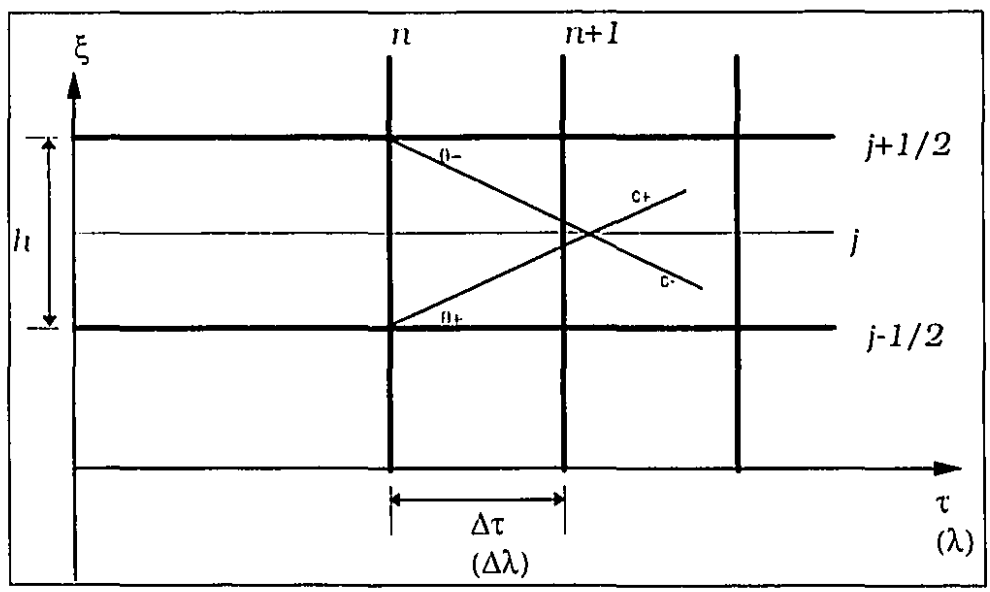

Figure 41. Domain of dependence

F.1 Lagrangian formulation based on Lagrangian-time

In figure 41 the stability condition is set so that the distance Δx traveled by a fluid particle at j during the time interval $\Delta\tau$ does not go beyond the point where the characteristic lines issued from both limiting corners of the cell cross the j^{th} streamline. (The two characteristic lines will not necessarily cross the j^{th} streamline at the same point)

For the C+ line:

$$\theta^{+} = \theta + \mu \ , \tag{F.1}$$

where

$$\theta = \tan^{-1}\frac{v}{u} \ , \tag{F.2}$$

$$\mu = \sin^{-1}\frac{1}{M} \ , \tag{F.3}$$

and

$$d\xi = \rho u l z \ , \tag{F.4}$$

where z is the system width and is equal to one in two-dimensional formulation.

From the geometry of figure 41 we write

$$\tan\theta^{+} = \frac{h}{2\Delta x} \ , \tag{F.5}$$

from which

$$\Delta x = \frac{h}{2\tan(\theta+\mu)_j} = \frac{d\xi}{\rho u 2\tan(\theta+\mu)_j} \ , \tag{F.6}$$

and

$$\Delta\tau = \frac{h\,\mathrm{CFL}}{2u_j\tan(\theta+\mu)_j} = \frac{d\xi\,\mathrm{CFL}}{2\rho u_j^2\tan(\theta+\mu)_j} \ , \tag{F.7}$$

where CFL is the stability condition and is always selected smaller than one in order to satisfy the condition that $\Delta\tau$ (or Δx) computed from equation (F.6) or (F.7) lies inside the domain influenced by the characteristic lines (C+ and C-).

F.2 Lagrangian formulation based on Lagrangian-distance

The same considerations apply to the Lagrangian formulation based on Lagrangian-distance, except that we now compute a distance interval instead of a time interval. This takes the following form:

$$\lambda = \Delta\tau \mathbf{V} = \Delta\tau\sqrt{u^2 + v^2} = \Delta\tau \frac{u}{\cos\theta} . \tag{F.8}$$

Replacing from equation (F.8) in (F.7) we get:

$$\Delta\lambda = \frac{d\xi \mathrm{CFL}}{2\rho u_j \tan(\theta + \mu)_j \cos\theta_j} . \tag{F.9}$$

BIBLIOGRAPHY

1. Anderson John D., Jr., Modern compressible flow with historical perspective, *McGraw Hill, 1991.*
2. Bach G. G., Applied mathematics, *McGill University, Mechanical Engineering Dept., course notes, 1993.*
3. Bach G. G., Numerical analysis, *McGill University, Mechanical Engineering Dept., course notes, 1993.*
4. Bronwell Arthur, Advanced Mathematics in Physics and Engineering, *McGraw Hill, 1953.*
5. Courant R. and Friedrichs K. O., Supersonic flow and shock waves, *Interscience Publishers Inc., New York, 1948.*
6. Eidelman Shmuel, Colella Philip and Shreeve Raymond P., Application of the Godunov method and its second order extension to cascade flow modeling, *AIAA Journal, vol 22, No. 11, p1609, 1984.*
7. Glatz Harland M. and Wardlaw Andrew B., A higher-order Godunov scheme for steady supersonic gas dynamics, *Journal of Computational Physics 58, pp 157-187, 1984.*
8. Hui W. H. and van Roessel H. J., Unsteady three dimensional flow theory via material functions, *NATO AGARD CP-386, paper #S1, 1985.*
9. Hui W. H. and Zhao Y. C., A generalized Lagrangian method for solving the steady Euler equations, *Second North American-Soviet Workshop on Computational Aerodynamics, Concordia University, Montréal, Canada, 1991.*
10. Jeffrey Alan, Mathematics for engineers and scientists, *Van Nostrand Reinhold (U. K.) Co. Ltd, 1989.*

11. Loh C. Y. and Hui W. H., A new Lagrangian method for steady supersonic flow computation, Part 1, Godunov scheme, *Journal of computational physics, vol. 89, No. 1, pp 207-240, 1990.*
12. Loh C. Y. and Hui W. H., Lagrangian Random choice method for steady two dimensional Supersonic/Hypersonic flow, *AIAA Journal, vol 31, p2193, 1993.*
13. Mateescu D. and Lauzon M., An explicit Euler Method for internal flow computation, *Computers and experiments in fluid flow, Springer Verlag Berlin, 1989, pp41-50.*
14. Mateescu D., High speed aerodynamics, *McGill University, Mechanical Engineering Dept., Course Notes, 1993.*
15. Mateescu D., Computational aerodynamics, *McGill University, Mechanical Engineering Dept., Course Notes, 1993.*
16. Mateescu D., *Private Communications, 1993.*
17. Newman B. G., Low speed aerodynamics, *McGill University, Mechanical Engineering Dept., Course Notes, 1993.*
18. Ni Ron-Ho, A Multiple-Grid Scheme for solving the Euler eqations, *AIAA Journal, vol 20, No. 11, p1565, 1982.*
19. Oswatitsch Klaus, Gas Dynamics, *New York Academic press, 1956.*
20. Roache Patrick J., Computational fluid dynamics, *Hermosa Publishers, 1970.*
21. Rutherford Aris, Vectors, tensors and the basic equations of fluid mechanics, *Prentice Hall Inc, 1962.*
22. Saad Michel A., Compressible fluid flow, 1985.
23. Shapiro Asher H., The dynamics and thermodynamics of compressible fluid flow, *the Ronald press company, New York, 1954.*
24. Sokolnikoff Ivan S., Higher Mathematics for engineers and Physicists, *McGraw Hill, 1966.*

25. Van Roessel H. J. and Hui W. H., A Lagrangian formulation for steady three-dimensional Newton-Busemann flow, *Journal of Applied Mathematics and Physics (ZAMP), vol. 40, pp 677-710, 1989.*

26. Woodward Paul and Collella Philip , Review article, the numerical simulation of two dimensional fluid flow with strong shocks, *Journal of computational physics 54, pp 115-173, 1984.*

27. Yang J. Y. and Hsu C. A., Solution of the steady Euler Equations in a Generalized Lagrangian formulation. *AIAA Journal, vol 31, No. 2, 1993.*

28. Yang J. Y. and Hsu Chiang-An, Numerical experiments with nonoscillatory schemes using Eulerian and new Lagrangian formulations, *Computers & Fluids Journal, vol 22, No. 2/3, 1992.*

29. Yang J. Y., Chang S. H. and Hui W. H., New Lagrangian method for steady supercritical shallow water flow computation, *Computer Methods in Applied Mechanics and Engineering, vol 104, pp 333-355, 1993.*

30. Batchelor George Keith, An introduction to fluid dynamics, *Cambridge University Press, 1967.*